creative commons
COMMONS DEED

저작자표시-비영리-변경금지 2.0 대한민국

이용자는 아래의 조건을 따르는 경우에 한하여 자유롭게

- 이 저작물을 복제, 배포, 전송, 전시, 공연 및 방송할 수 있습니다.

다음과 같은 조건을 따라야 합니다:

저작자표시. 귀하는 원저작자를 표시하여야 합니다.

비영리. 귀하는 이 저작물을 영리 목적으로 이용할 수 없습니다.

변경금지. 귀하는 이 저작물을 개작, 변형 또는 가공할 수 없습니다.

- 귀하는, 이 저작물의 재이용이나 배포의 경우, 이 저작물에 적용된 이용허락조건을 명확하게 나타내어야 합니다.
- 저작권자로부터 별도의 허가를 받으면 이러한 조건들은 적용되지 않습니다.

저작권법에 따른 이용자의 권리는 위의 내용에 의하여 영향을 받지 않습니다.

이것은 이용허락규약(Legal Code)을 이해하기 쉽게 요약한 것입니다.

Disclaimer

dCollection

의학박사 학위논문

Search for molecular features and pathogenic pathways in tuberous sclerosis complex-associated renal cell carcinoma

결절성 경화증 연관 신세포암의 분자유전학적 특성 및 발생기전 연구

2019 년 8 월

서울대학교 대학원

의학과 병리학 전공

박 정 환

결절성 경화증 연관 신세포암의 분자유전학적 특성 및 발생기전 연구

지도교수 문 경 철

이 논문을 의학박사 학위논문으로 제출함

2019 년 4 월

서울대학교 대학원

의학과 병리학 전공

박 정 환

박정환의 박사 학위논문을 인준함

2019 년 7 월

위 원 장 강 개 호 (인)

부위원장 문 경 철 (인)

위 원 유 형 호 (인)

위 원 곽 철 (인)

위 원 임 소 덕 (인)

Search for molecular features and pathogenic pathways in tuberous sclerosis complex-associated renal cell carcinoma

by

Jeong Hwan Park, M.D.

Director: Prof. Kyung Chul Moon, M.D., Ph.D.

A thesis submitted to the Department of Pathology in partial fulfillment of the Requirements for the Degree of Doctor of Philosophy in Medicine (Pathology) at Seoul National University College of Medicine

July 2019

Doctorial committee:

Professor Gyeong Hoon Kang, Chairperson

Professor Kyung Chul Moon, Vice Chairperson

Professor Chesi Kwak

Professor SEONG HO YOO

Professor SOOUG LIM

Abstract

Background. Tuberous sclerosis complex-associated renal cell carcinoma (TSC-RCC) has distinct clinical and histopathologic features and is considered a specific subtype of RCC. The genetic alterations of *TSC1* or *TSC2* are responsible for the development of TSC. In this study, we assessed the mTOR pathway activation and aimed to evaluate molecular characteristics and pathogenic pathways of TSC-RCC.

Methods and results. Two cases of TSC-RCC, one from a 31-year-old female and the other from an 8-year-old male, were assessed. The mTOR pathway activation was determined by immunohistochemistry. The mutational spectrum of both TSC-RCCs were evaluated by whole exome sequencing (WES) and pathogenic pathways were analysed. Differentially expressed genes were analysed by NanoString Technologies nCounter platform. The mTOR pathway activation and the germline mutations of *TSC2* were identified in both TSC-RCC cases. The WES revealed several cancer gene alterations. In Case 1, genetic alterations of *CHD8*, *CRISPLD1*, *EPB41L4A*, *GNA11*, *NOTCH3*, *PBRM1*, *PTPRU*, *RGS12*, *SETBP1*, *SMARCA4*, *STMN1* and *ZNRF3* were identified. In Case 2, genetic alterations of *IWS1* and *TSC2* were identified. Further, putative pathogenic pathways included chromatin

remodelling, G protein-coupled receptor, Notch signalling, Wnt/β-catenin, PP2A and the microtubule dynamics pathway in Case 1, and mRNA processing and the PI3K/AKT/mTOR pathway in Case 2. Additionally, the *ALK* and *CRLF2* mRNA expression was upregulated and *CDH1*, *MAP3K1*, *RUNX1*, *SETBP1* and *TSC1* mRNA expression was downregulated in both TSC-RCCs.

Conclusions. We present mTOR pathway activation and molecular characteristics with pathogenic pathways in TSC-RCCs, which will advance our understanding of the pathogenesis of TSC-RCC.

Keywords: molecular characterization, pathogenesis, tuberous sclerosis complex-associated renal cell carcinoma, whole exome sequencing

Student number: 2012-30552

Contents

List of Tables

List of Figures

Introduction

Renal cell carcinoma (RCC) is one of the most fatal genitourinary tumours and accounts for approximately 90% of renal cancers (1). Histopathologic features and molecular studies have identified and classified various subtypes of RCC (2,3). These subtypes include clear cell RCC (CCRCC), papillary RCC (PRCC), chromophobe RCC (ChRCC), MiT family translocation RCC, and clear cell papillary RCC. Additionally, syndrome associated hereditary renal cell tumours, including Von Hippel-Lindau syndrome, hereditary papillary RCC and tuberous sclerosis, have been identified. The National Cancer Data Base revealed 5-year survival rates of 80.9% in stage I, 73.7% in stage II, 53.3% in stage III and 8.2% in stage IV kidney cancer patients (4). Various aspects of the treatment for advanced RCC and metastatic RCC have been studied, and target therapy and immunotherapy have showed considerable improvement in patient survival (5-7).

Tuberous sclerosis complex-associated RCC (TSC-RCC) is an emerging subtype of RCC (8,9). TSC showed autosomal dominant inheritance and was characterized by multisystem disorders, including epilepsy, developmental delay, angiofibromas, hypomelanotic macules, cortical dysplasias, lymphangioleiomyomatosis and angiomyolipoma (AML) (10,11).

The disease is caused by alterations in *TSC1* or *TSC2* genes, which encode hamartin and tuberin, respectively (10). Studies of TSC-RCC from multiple institutions have revealed the clinical and histopathologic features of TSC-RCC (8,9). Clinically, TSC-RCC is characterized by an association with TSC, female predominance, early age of onset and indolent clinical outcomes. Histopathologically, TSC-RCC has been classified according to several distinct morphologies, including renal angiomyoadenomatous tumor (RAT)-like, TSC-associated papillary RCC, chromophobe-like or hybrid oncocytic/chromophobe tumor (HOCT)-like, eosinophilic/macrocystic and unclassified RCC.

Cancer genomics has been greatly expanded our knowledge of cancer biology. In kidney cancers, CCRCC, PRCC and ChRCC were analysed, and important genomic events and pathways were elucidated (12-14). Moreover, actionable targets for RCC have been identified, and patients with those alterations have been enrolled in clinical trials (15,16). As precision medicine has been initiated in earnest, unveiling the genomic landscape of cancer has progressed, resulting in promising improvements in treatment modalities and patient prognoses (17,18). Additionally, studies of rare but specific genetic alterations, such as those in TSC-RCC, will advance our understanding of cancer biology and the discovery of novel cancer-related genes.

In this study, we assessed the activation of the mTOR pathway and the genetic alterations in two cases of TSC-RCC by immunohistochemistry and whole exome sequencing (WES). Additionally, we analysed mRNA expression of cancer genes. We aimed to evaluate the mutation spectrum of both patients and search for the genetic basis of the pathogenesis and actionable targets of TSC-RCC.

Materials and methods

Patient selection and clinicopahtologic review

We retrospectively reviewed all RCCs surgically removed by radical or partial nephrectomy between January 1, 2009 and December 31, 2014 at Seoul National University Hospital. We reviewed the medical records to identify TSC patients and identified two cases of TSC-RCC. Each TSC-RCC was evaluated with regard to the clinical and histopathologic features, such as history of epilepsy, RCC histologic type (19), WHO/ISUP grade (20, 21) and the stage of the tumour (22). Disease progression was determined based on the clinical and radiographic findings and the patients' medical records. This study was approved by the Institutional Review Board of Seoul National University Hospital.

Immunohistochemistry

We performed immunohistochemistry on a representative slide from TSC-RCC cases (Table 1). For the differential diagnosis, we assessed pan-cytokeratin, HMB-45, Melan A, CD10, CK7 and c-kit immunoreactivity. To

evaluate mTOR pathway activation, we assessed phospho-mTOR immunoreactivity. Immunohistochemical staining was performed using autostainers for each antibody. The binding of the primary antibody was detected using a detection kit, according to the manufacturer's instructions.

Table 1. Antibodies used for immunohistochemistry

Antibody	Dilution	Source	Detection kit	Autostainer
Pan-cytokeratin	1:300	DAKO	DAKO EnVision Flex kit	Dako Autostainer Link 48 (DAKO Corp., Carpintera, CA, USA)
CD10	RTU	Leica Biosystems	Optiview DAB IHC detection kit	Ventana BenchMark XT (Ventana Medical Systems Inc., Tucson, AZ, USA)
CK7	1:300	DAKO	Optiview DAB IHC detection kit	Ventana BenchMark XT (Ventana Medical Systems Inc., Tucson, AZ, USA)
c-kit	1:300	DAKO	Optiview DAB IHC detection kit	Ventana BenchMark XT (Ventana Medical Systems Inc., Tucson, AZ, USA)
HMB-45	1:200	DAKO	DAKO EnVision Flex kit	Dako Autostainer Link 48 (DAKO Corp., Carpintera, CA, USA)
Melan A	1:500	Cell Marque	Bond polymer refine detection kit	Bond-Max Autostainer (Leica Microsystems, Buffalo Grove, IL, USA)
phospho-mTOR	1:50	Cell Signaling Technology	UltraView Universal DAB detection kit	Ventana BenchMark XT (Ventana Medical Systems Inc., Tucson, AZ, USA)

Tissue sample identification and DNA extraction

Normal and cancer tissue were identified by reviewing each haematoxylin and eosin slide. The normal tissue was obtained far from the cancer tissue area. We carefully marked the area of normal and cancer tissues for matching with formalin-fixed, paraffin-embedded (FFPE) tissue block. For each FFPE tissue block, 3 cores of 4 mm in diameter were punched, and DNA was extracted using the GeneRead DNA FFPE Kit (Qiagen, Hilden, Germany) according to the manufacturer's instructions. Samples were mixed with RNase-free water, buffer FTB and proteinase K, followed by incubation and centrifugation. The lysates were transferred to a QIAamp MinElute column and centrifuged. DNA was eluted with Buffer ATE, incubated and centrifuged.

Whole exome sequencing

We checked the quality of DNA based upon an OD 260/280 ratio of 1.8-2, by 1% agarose gel electrophoresis and PicoGreen® dsDNA Assay (Invitrogen). WES was performed using HiSeq 2500 sequencing system (Illumina) using SureSelect All Exon kit V4 (Agilent). SureSelect sequencing libraries were prepared according to the manufacturer's instructions. Genomic

DNA (200 ng) in 50 μL EB buffer was fragmented to a median size of 150 bp using Covaris-S2 instrument (Covaris). The adapter ligated DNA was amplified by PCR and the quality of the PCR products was assessed by capillary electrophoresis (Bioanalyzer, Agilent). The captured library was amplified to add index tags using Herculase II Fusion DNA Polymerase (Finnzymes). After qPCR by SYBR Green PCR Master Mix (Applied Biosystems), we combined libraries with index tagged in equimolar amounts. The flow cell was loaded onto a HiSeq 2500 sequencing system, and clustering and sequencing with a 2x100 bp read length was performed.

Alignment and germline variant and somatic mutation calling

Sequence QC was performed using FastqQC 0.11.2 (23), and was mapped to human reference genome sequence NCBI b37 using BWA 0.7.12 (24). BAM files were realigned using the Genome Analysis Toolkit (GATK) 3.3 IndelRealigner (25), and base quality scores were recalibrated using the GATK base quality recalibration tool. For germline variant calling, GATK's UnifiedGenotyper tool 3.3 was used. To filter potential errors, GATK's Variant Quality Score Recalibration was performed based on hapmap 3.3, NCBI Variation Database (dbSNP138), 1000 Genomes and Omni 2.5M SNP

chip array. Functional information of variants was annotated using SnpEff 4.1(GRCh 37.75) (26). Somatic mutations of single nucleotide variant (SNV) and small indel were detected using MuTect v1.1.7 (27) and Strelka v1.0.14 (28) with default parameter setting. The functional information of variants was annotated using Oncotator v1.5.1.0 (29) with the GRCh37.75 reference set (Figure 1).

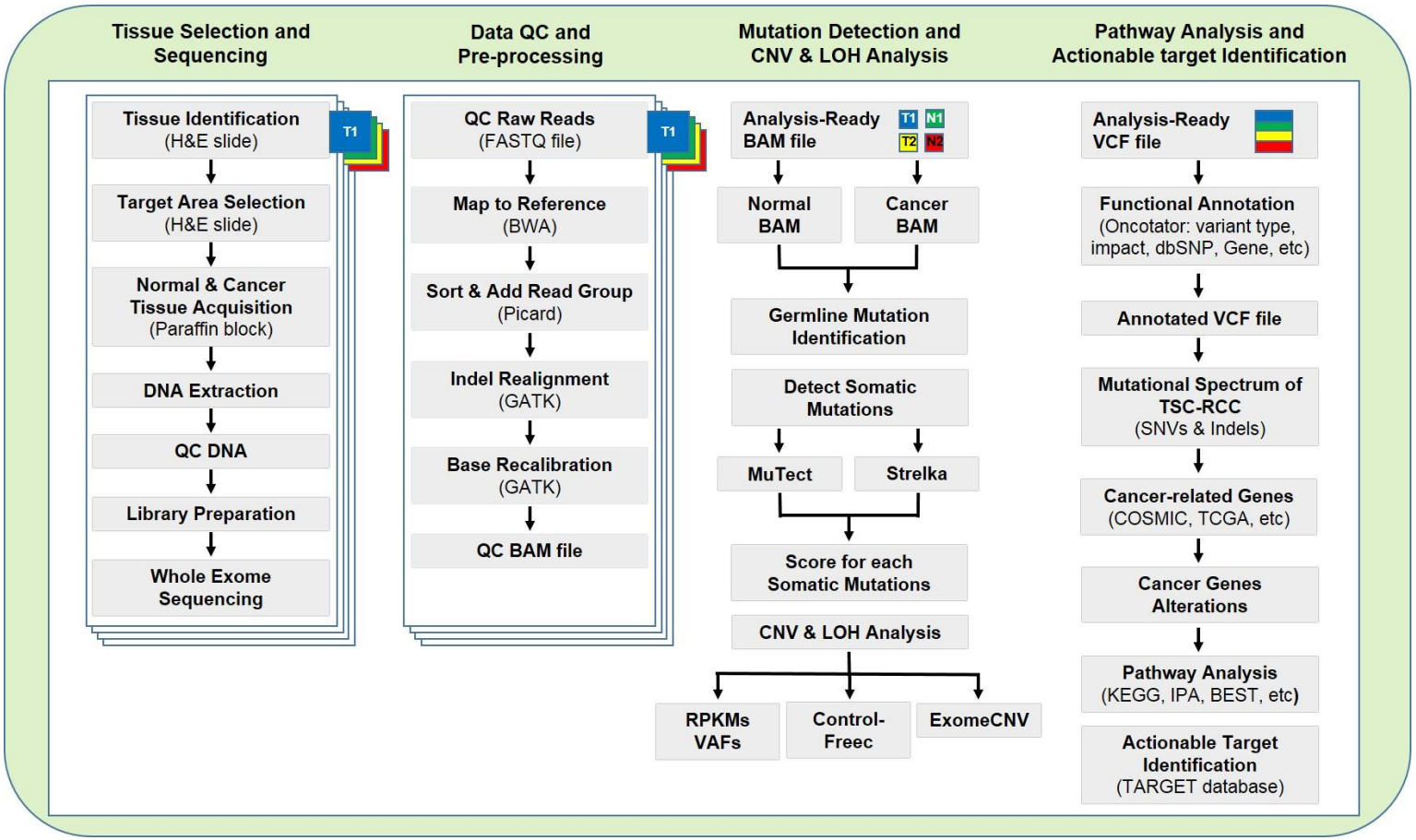

Figure 1. Bioinformatic analysis workflow of whole exome sequencing data

Identification and evaluation of genetic alterations

The mutations with allele depth of ≥10x, variant allele frequency (VAF) of ≥1% and no strand bias were included. Germline mutations of *TSC1* or *TSC2* were assessed. Somatic mutations were identified by comparing normal and cancer tissue BAM files and using MuTect and Strelka methods. For somatic mutation analysis, total score of ≥2 by adding MuTect and Strelka score, variant classification score of ≤4 (Table 2) and VAF of ≥5% were included. The predicted protein function of altered genes were assessed using PolyPhen-2 (http://genetics.bwh.harvard.edu/pph2) (30), MutationAssessor (http://mutationassessor.org/r3) (31) and MutationTaster (http://mutationtaster.org) (32). We manually checked each genetic alterations using Integrative Genomics Viewer.

Table 2. Variant classification score

Variant classification	Score
De novo Start OutOfFrame	0
Nonsense Mutation	0
Nonstop Mutation	0
Missense Mutation	1
De novo Start InFrame	1
In Frame Del / Ins	1
Frame Shift Del / Ins	2
Frame Shift Sub	2
Start Codon SNP	3
Start Codon Del / Ins	3
Start Codon DNP / TNP / ONP	3
Stop Codon SNP / Del / Ins	3
Stop Codon DNP / TNP / ONP	3
Splice Site	4
Splice Site SNP / Del / Ins	4
Splice Site DNP / TNP / ONP	4
Splice Site	4
miRNA	4
Silent	5
3UTR	6
5UTR	6
Intron	7
5Flank	8
3Flank	8

Variant classification	Score
Non-coding Transcript	9
IGR	20
TX-REF-MISMATCH	100

Cancer-related genes

The cancer-related gene list is constructed by referring to several articles (12-14, 33-35), Catalogue Of Somatic Mutations In Cancer (COSMIC) database v81 (http://cancer.sanger.ac.uk/cosmic) (36), The Cancer Genome Atlas (TCGA) database (http://cancergenome.nih.gov) (12,13), cBioPortal database version 1.4.3 (http://www.cbioportal.org) (37,38), Kyoto Encyclopedia of Genes and Genomes (KEGG) pathway genes (pathways in cancer and pathways of specific cancer types) (http://www.genome.jp/kegg) (39,40) and commercially available cancer panels (Ion Torrent comprehensive cancer panel, Oncomine cancer panel and nCounter® pan-cancer pathways panel) (Table 3).

Table 3. Cancer-related gene lists

Driver genes		KEGG_TSG_OG		COSMIC_TSG_OG	
ABL1	PIK3R1	ABL1	RARA	ABI1	KMT2A
ACVR1B	PPP2R1A	AFF1	RARB	ABL1	KRAS
AKT1	PRDM1	AKT1	RASSF1	ABL2	LEF1
ALK	PTCH1	AKT2	RB1	ACKR3	LZTR1
APC	PTEN	AKT3	REL	ACVR1	MDM2
AR	PTPN11	ALK	RET	AFF1	MDM4
ARID1A	RB1	APC	RUNX1	AFF3	MECOM
ARID1B	RET	AR	RUNX1T1	AFF4	MEN1
ARID2	RNF43	ASPSCR1	RUNXX1T1	AKAP9	MET
ASXL1	RUNX1	ATF1	SHH	AKT1	MLLT1
ATM	SETD2	BAX	SIRT3	AKT2	MLLT3
ATRX	SETBP1	BCL6	SIRT6	ALDH2	MPL
AXIN1	SF3B1	BCR	SLC45A3	ALK	MTOR
B2M	SMAD2	BRAF	SMAD2	AMER1	MYC
BAP1	SMAD4	BRCA1	SMAD4	APC	MYCN
BCL2	SMARCA4	BRCA2	SMO	AR	MYD88
BCOR	SMARCB1	CCDC6	SPI1	ARHGAP26	NAB2
BRAF	SMO	CCND1	SS18	ARHGEF12	NCOR2
BRCA1	SOCS1	CDK4	SSX1	ARID1A	NFKB2
BRCA2	SOX9	CDKN1B	SSX2	ARID1B	NOTCH1
CARD11	SPOP	CDKN2A	SSX2B	ARID2	NOTCH2
CASP8	SRSF2	CEBPA	TAF15	ARNT	NRAS
CBL	STAG2	CTNNB1	TCF3	ASPSCR1	PALB2
CDC73	STK11	DCC	TFE3	ASXL1	PBRM1
CDH1	TET2	DDIT3	TFG	ATM	PDGFB
CDKN2A	TNFAIP3	DDX5	TGFBR2	ATP1A1	PDGFRA
CEBPA	TRAF7	EGFR	TLX1	BAP1	PIK3CA
CIC	TP53	ELK4	TLX3	BCL2	PML
CREBBP	TSC1	EML4	TMPRSS2	BCL3	PRKACA
CRLF2	TSHR	ERBB2	TP53	BCL5	PTEN
CSF1R	U2AF1	ERG	TPM3	BCL6	PTK6

Driver genes		KEGG_TSG_OG		COSMIC_TSG_OG	
CTNNB1	VHL	ETV1	TPR	BCL7A	PTPN11
CYLD	WT1	ETV4	VHL	BCL9	PTPN13
DAXX	CCND1	ETV6	WHSC1	BCOR	RARA
DNMT1	CDKN2C	ETV7	WT1	BCR	RB1
DNMT3A	IKZF1	EWSR1	ZBTB16	BRAF	RBM10
EGFR	LMO1	FEV		BRCA1	REL
EP300	MAP2K4	FGFR3		BRCA2	RET
ERBB2	MDM2	FH		CALR	ROS1
EZH2	MDM4	FHIT		CASP8	RUNX1
FAM123B	MYC	FLCN		CBL	RUNX1T1
FBXW7	MYCL1	FLI1		CBLB	SDHA
FGFR2	MYCN	FLT3		CCND1	SETD2
FGFR3	NCOA3	FOXO1		CDC73	SH2B3
FLT3	NKX2-1	FUS		CDK4	SMAD2
FOXL2	SKP2	HRAS		CDK6	SMAD3
FUBP1		IGH		CDKN1B	SMAD4
GATA1		KIT		CDKN2A	SOCS1
GATA2		KMT2A		CDKN2C	STAT3
GATA3		KRAS		CHD4	SYK
GNA11		LMO2		CHEK2	TBX3
GNAQ		MAF		CTCF	TET1
GNAS		MDM2		CTNNB1	TET2
H3F3A		MECOM		CXCR4	TGFBR2
HIST1H3B		MEN1		CYLD	TP53
HNF1A		MET		DICER1	TRRAP
HRAS		MITF		DNMT3A	TSC1
IDH1		MLH1		ERBB2	TSC2
IDH2		MLLT1		ERBB3	USP8
JAK1		MLLT3		ERBB4	VHL
JAK2		MSH2		ERCC2	XPA
JAK3		MSH3		EZH2	XPC
KDM5C		MSH6		EZR	ZFHX3

Driver genes	KEGG_TSG_OG	COSMIC_TSG_OG
KDM6A	MYC	FAT1
KIT	MYCN	FAT4
KLF4	NCOA4	FLT3
KRAS	NKX3-1	FOXO1
MAP2K1	NR4A3	FOXO3
MAP3K1	NRAS	FOXO4
MED12	NTRK1	FOXP1
MEN1	PAX3	FUS
MET	PAX5	GATA1
MLH1	PAX7	GATA2
MLL2	PAX8	GATA3
MLL3	PBX1	HIF1A
MPL	PDGFA	HLF
MSH2	PDGFRA	HMGA2
MSH6	PDGFRB	HOXA11
MYD88	PIK3CA	HOXA13
NCOR1	PIK3CB	HOXA9
NF1	PIK3CD	HOXC11
NF2	PIK3CG	HOXC13
NFE2L2	PIK3R1	HOXD11
NOTCH1	PIK3R2	HOXD13
NOTCH2	PIK3R3	HRAS
NPM1	PIK3R5	IDH1
NRAS	PIKCCG	IDH2
PAX5	PML	IKZF1
PBRM1	PPARG	IRF4
PDGFRA	PRCC	JAK2
PHF6	PTCH1	KIT
PIK3CA	PTEN	KLF4

CNV detection methods

After pre-processing the sequenced reads, we listed large-scale CNVs using read depth and variant allele fraction (VAF) information. For all tumor and normal alignment data, read depth data were calculated using GATK DepthOfCoverage (25), and variants were called using GATK HaplotypeCaller (25). For all tumor and normal samples, log2(RPKM [Reads Per Kilobase Million]) were calculated as a measure to calculated the normalized coverage information. After calculating the RPKMs and VAFs for all possible genomic coordinates, the RPKM and VAF information were uploaded to the Integrative Genomics Viewer (41,42). Large-scale CNVs were then visually inspected.

Control-Freec

We use default option of Control-FREEC(6.4) for copy number variant (43). And then, we created a config file that the window size of the general record is setted as 500 and bam files is seted to each sample and control records. Analysis result to CNV type is classified based on genome ploidy value 2; below 2 is loss and above 2 is gain.

ExomeCNV

We combined two VCF (Variant Calling Format) file of each normal-tumour paired sample by GATK (Genome Analysis Toolkit) CombineVariants. From the combined VCF file, we created preprocessing BAF (B Allele Frequency) file which contains chromosome, position, coverage and baf column. And then, LOH analysis was performed by R Exome CNV v1.4 (44). Calling LOH on each heterozygous position was performed by function LOH.analyze with the value of alpha is 0.0001 and the statistical method is two.sample.prop. The function multi.LOH.analyze was performed to calling LOH on each segment with the value of test.alpha is 0.0001 and the statistical method is variance.f. We visualized BAF with function do.plot.loh and marked it green color for LOH region.

Sanger sequencing

We performed Sanger sequencing for the validation of cancer genes. Genomic DNA samples were extracted using an MG Clinic SV kit (Doctor Protein). Target gene specific primer pairs and Dr. MAX DNA Polymerase (Doctor Protein Inc, Korea) were utilized for PCR reactions. PCR products

were purified using Millipore plate MSNU030 (Millipore SAS, Molsheim, France). The products were Sanger-sequenced with the BigDye terminator v3.1 sequencing kit and a 3730xl automated sequencer (Applied Biosystems, Foster City, CA). Nucleotide sequences were determined on both strands. Nucleotide sequence data were analysed with Variant reporter computer software version 1.1 (Applied Biosystems, Foster City, CA).

Droplet digital PCR

Droplet digital PCR (dd-PCR) was performed using QX200^{TM} Droplet Digital^{TM} PCR system (Bio-Rad Laboratories, Hercules, CA, USA) to validate cancer genes alterations in TSC-RCC Case 1. DNA was extracted from unstained slides and FFPE blocks from cancer area. The customized probes were used and dd-PCR was performed according to the manufacturer's protocol. Droplets were generated using the QX200 droplet generator and read in the QX200 droplet reader. To avoid potential false positive results, we validated designed dd-PCR probes using normal tissue from TSC-RCC Case 1. After verifying that no positive calls in normal tissue, we proceeded dd-PCR to validate genetic alterations in TSC-RCC Case 1. The results were

analysed using the Quantasoft software version 1.3.2.0 (Bio-Rad Laboratories).

Pathway analysis

For the analysis of pathogenic pathways for each TSC-RCC, we selected cancer genes according to the following criteria: depth (≥10x), VAF (≥20%), score (≥3), no strand bias, altered function (≥1 prediction method), tumour suppressor genes (TSGs) or oncogenes (OGs) (34). We used KEGG pathway maps (http://www.genome.jp/kegg/pathway.html) (39,40), and Ingenuity pathway analysis (IPA) (http://www.ingenuity.com/products/ipa) (45) for pathway analysis. Additionally, we used STRING (http://string-db.org) (46) for assessment of protein-protein interaction networks.

mRNA expression analysis

Total RNA was extracted using an eCube RNA Mini Kit (Philekorea Technology, Seoul, Korea). RNA yield and purity were assessed using a DS 11 Spectrophotometer (Denovix Inc, DE, USA). Total RNA (300 ng) was added to the sample preparation reaction in the available 5 μL volume. RNA

quality was verified using a Fragment Analyzer (Advanced Analytical Technologies, IA, USA). The digital multiplexed nanoString nCounter human mRNA expression assay (nanoString Technologies) was performed. The mRNA data analysis was performed using the nSolver software analysis. The mRNA profiling data was normalized using housekeeping genes.

Comparison with reported data and public database

We analysed the sequencing results with the COSMIC, TCGA, and cBioPortal database (12,13,36-38). Genetic alterations were compared to common RCCs (CCRCC, PRCC and ChRCC) sequencing data (12-14). Also, we compared our results to genetic data of TSC-associated papillary RCC (47) and molecular characteristics of eosinophilic/macrocystic RCC (48,49). Potential actionable targets were evaluated by matching molecular targets of FDA-approved drugs (50) and Tumor Alterations Relevant for GEnomics–driven Therapy (TARGET) database (http://www.broadinstitute.org/cancer/cga/target).

Results

Clinical features of TSC-RCC patients

The Case 1 patient was a 31-year-old female with a history of seizures from a young age who was clinically diagnosed with TSC for her facial angiofibromas and subependymal nodules. The patient had multiple renal masses, and one of them was diagnosed as AML. Upon follow-up, she visited the hospital for abdominal pain, and a 15.4 x 10.0 cm mass was detected in the right kidney. The Case 2 patient was an 8-year-old male with a history of seizures from12 months who was suspected to have TSC due to his facial angiofibromas. On work-up, multiple subependymal nodules and cortical tubers were identified. Additionally, a 5.2 x 7.1 x 6.0 cm mass was detected in the left kidney. Radical nephrectomy was performed on both patients.

Histopathologic features of TSC-RCC cases

The TSC-RCC Case 1 consisted of a 16.5 x 10.5 x 7.9 cm solid mass with haemorrhage and necrosis (Figure 2). The tumour showed sheet-like growth pattern and was composed of discohesive large atypical cells with

ample, light eosinophilic cytoplasm and vesicular nucleus with prominent nucleolus. The emperipolesis, neutrophilic infiltration and abscess as well as angiolymphatic invasion were identified. WHO/ISUP grade was 4 and pTNM stage was II (pT2bN0M0). The TSC-RCC Case 2 consisted of a 7.3 x 5.3 x 4.0 cm solid mass with focal cystic change (Figure 3). The tumour showed trabecular growth with atypical cells with plump, eosinophilic and granular cytoplasm. The tumour cells revealed vesicular and wrinkled nuclei with small nucleoli. The cysts showed hobnail pattern of cyst lining cells with plump eosinophilic granular cytoplasm. Additionally, the tumour revealed hyalinised stroma. The angiolymphatic invasion was identified. WHO/ISUP grade was 2 and pTNM stage was II (pT2aN0M0). Both cases had multiple renal AMLs. The Case 2 patient had multiple variable sized renal cysts lined by epithelial cells with plump eosinophilic cytoplasm, which was reported as histologic features of epithelial cysts in TSC (51) or cuboidal cells. Immunohistochemically, both cases were negative for myomelanocytic markers (HMB-45, Melan A) and positive for epithelial marker (pan-cytokeratin), suggesting RCC rather than epithelioid AML. Case 1 can be classified as unclassified RCC, and Case 2 as RCC with eosinophilic/macrocystic feature. Additionally, phospho-mTOR was positive in TSC-RCCs but not in adjacent unaffected renal parenchyma.

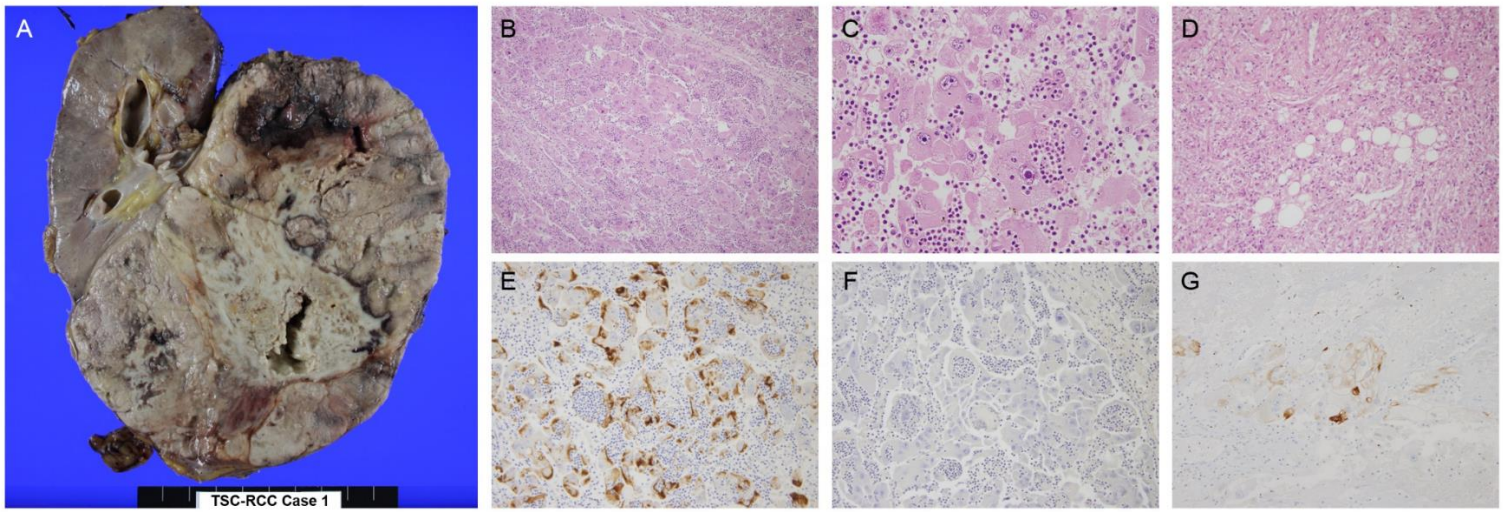

Figure 2. Pathologic features of TSC-RCC Case 1. (A) Macroscopic findings. (B-D) Histopathologic findings ((B) low power view, (C) high power view, (D) angiomyolipoma) and (E-G) immunohistochemical findings ((E) pan-cytokeratin, (F) HMB-45, (G) phospho-mTOR). Original magnification ×100 (B), ×200 (D-G), and ×400 (C).

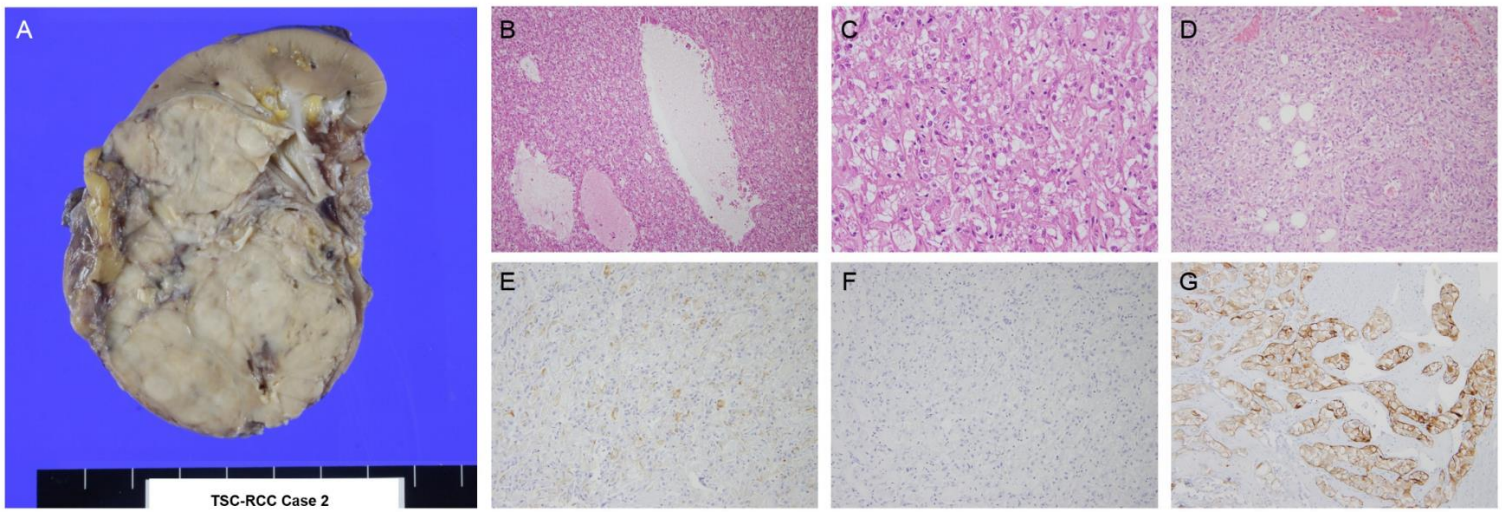

Figure 3. Pathologic features of TSC-RCC Case 2. (A) Macroscopic findings. (B-D) Histopathologic findings ((B) low power view, (C) high power view, (D) angiomyolipoma) and (E-G) immunohistochemical findings ((E) pan-cytokeratin, (F) HMB-45, (G) phospho-mTOR). Original magnification ×100 (B), ×200 (D-G), and ×400 (C).

Germline mutations of *TSC1* or *TSC2* genes in TSC-RCC cases

We regarded identical mutations on both normal and cancer tissues as germline mutations. In Case 1, a *TSC2* c.4707C>A (p.Tyr1569*) mutation was identified, and in Case 2, a *TSC2* c.2548+2T>G mutation was seen (Figure 4 and Table 4), which were stop gained effect and a splice donor variant, respectively.

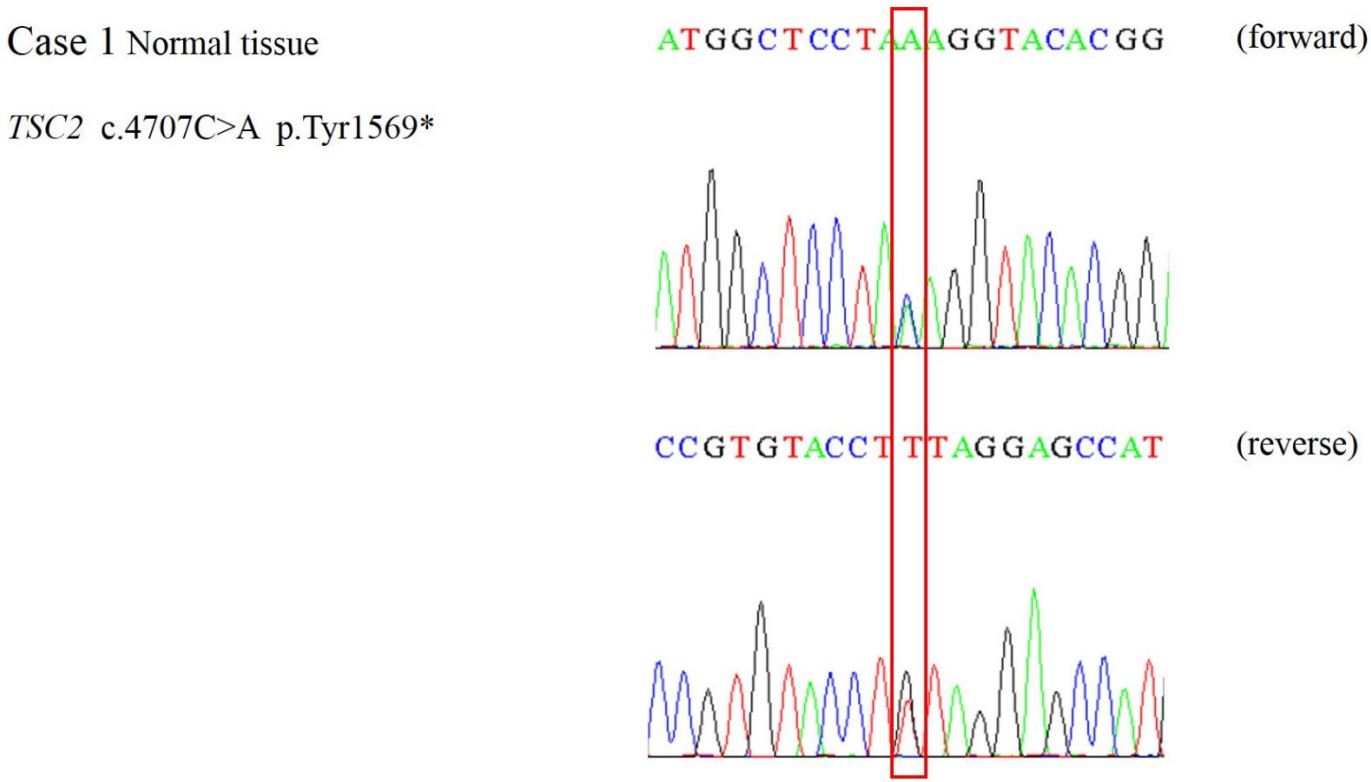

Figure 4. Germline mutations of *TSC1* or *TSC2* genes in TSC-RCC cases

Case 1 Tumor tissue

TSC2 c.4707C>A p.Tyr1569*

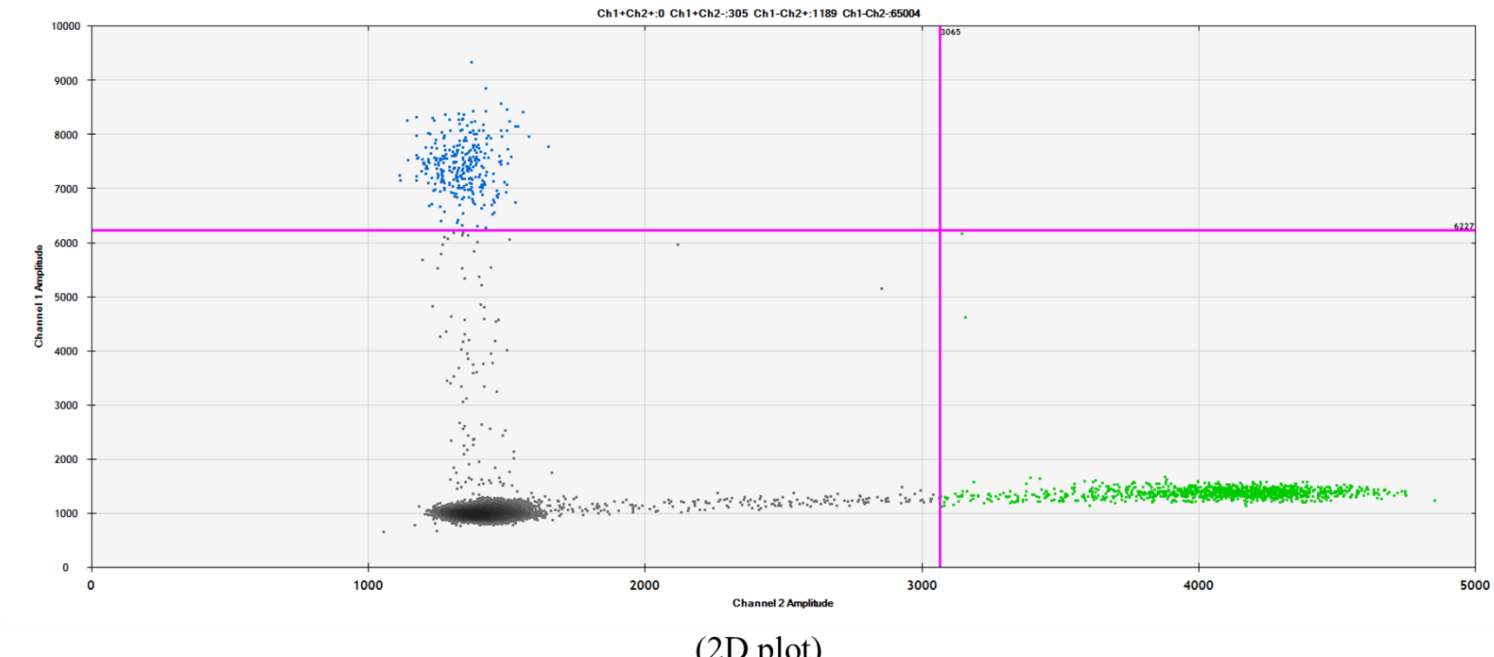

(2D plot)

Figure 4. Germline mutations of *TSC1* or *TSC2* genes in TSC-RCC cases

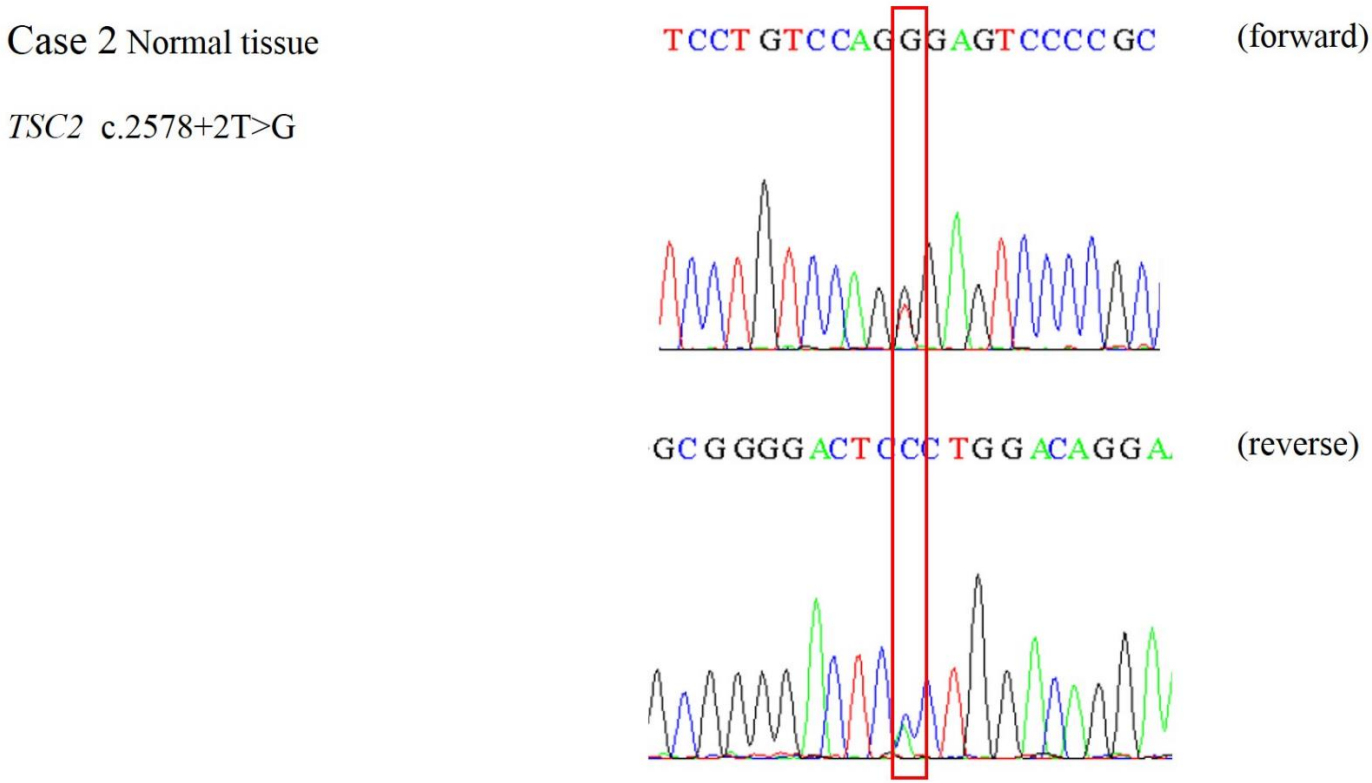

Figure 4. Germline mutations of *TSC1* or *TSC2* genes in TSC-RCC cases

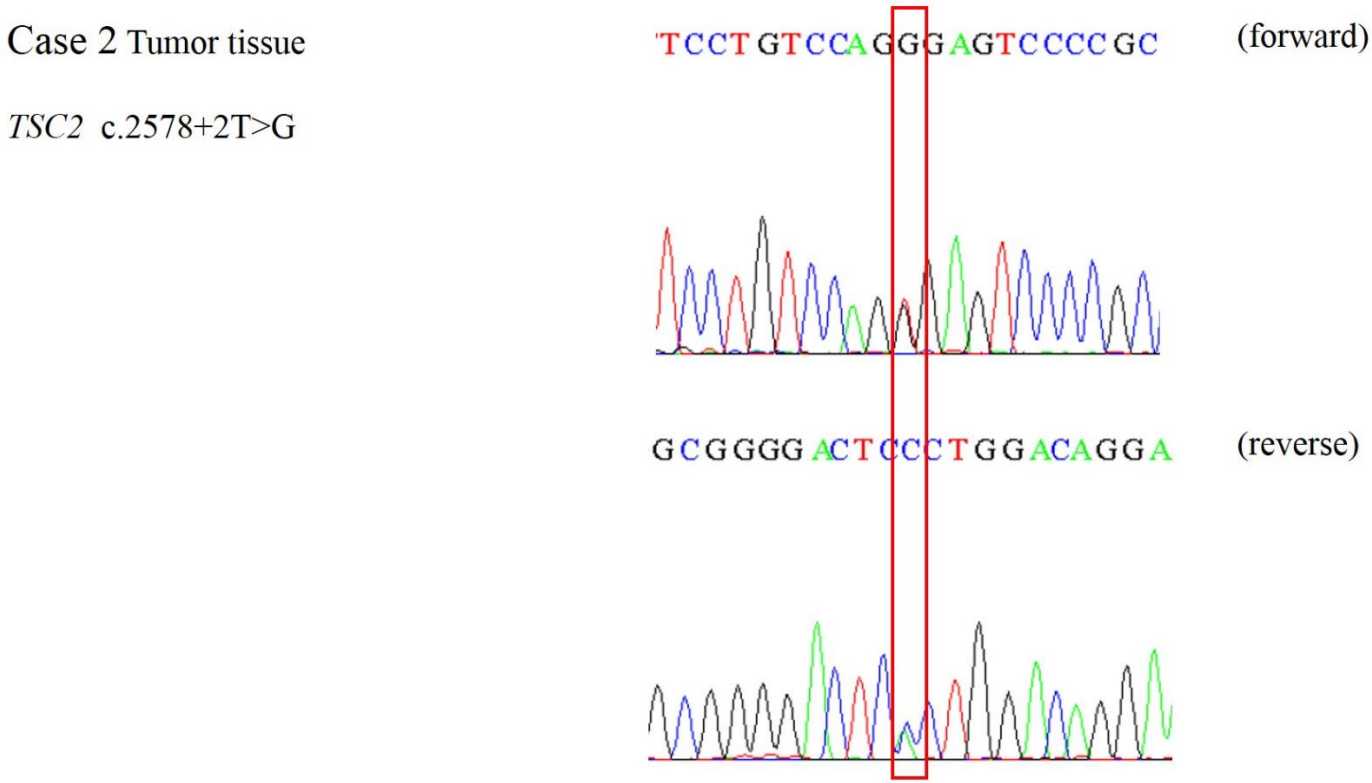

Figure 4. Germline mutations of *TSC1* or *TSC2* genes in TSC-RCC cases

Table 4. Germline mutations of *TSC1* or *TSC2* genes in two cases of TSC-RCC

Case	Gene	Reference	Alternate	Variant Type	Effect	Impact	HGVS.c	HGVS.p	1000G ASN Maf	VAF (%)	Validation[a]
1	*TSC2*	C	A	SNV	stop gained	HIGH	c.4707C>A	p.Tyr1569*	NA	45.35	+
2	*TSC2*	T	G	SNV	splice donor variant & intron variant	HIGH	c.2578+2T>G	.	NA	52.00	+

[a]Sanger sequencing was performed in normal tissues from both cases and tumour tissue from case 2. Droplet digital PCR was performed in tumour tissue from case 1.

Abbreviation: NA, not available; VAF, variant allele frequency

Somatic mutations and alterations of cancer-related genes in TSC-RCC cases

The somatic mutations of SNV or small indels were analysed (Figure 5). In Case 1, a total of 589 mutations (567 SNVs, 1 insertion and 21 deletions) were identified. In Case 2, a total of 258 mutations (257 SNVs and 1 deletions) were identified. Further, alterations of cancer-related genes were assessed. In Case 1, 72 cancer-related genes were identified (Figure 6A and table 5). There were 69 SNVs and 3 deletions, including 58 missense mutations, 6 nonsense mutations, 5 splice site SNVs, 2 in frame deletions and 1 frame shift deletion. In Case 2, we identified 32 altered cancer-related genes (Figure 6B and table 6). There were 31 SNVs and 1 deletion, including 23 missense mutations, 5 nonsense mutations, 3 splice site SNVs and 1 frame shift deletion.

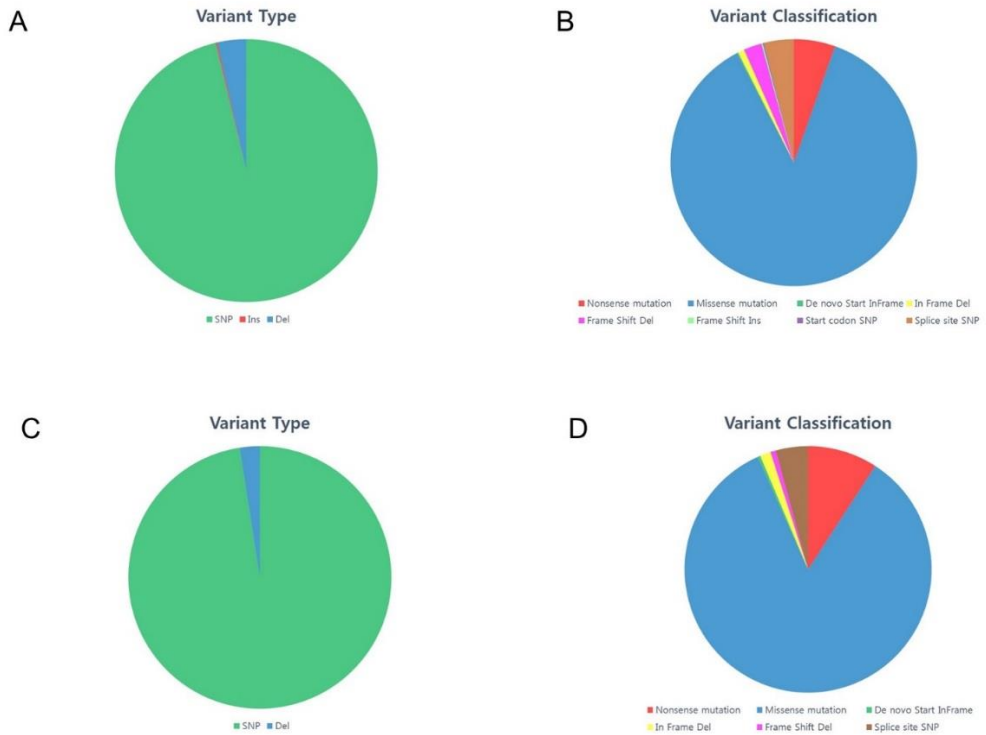

Figure 5. Mutational spectrum of TSC-RCC cases (A) Variant type and (B) Variant classification of TSC-RCC Case 1 and (C) Variant type and (D) Variant classification of TSC-RCC Case 2

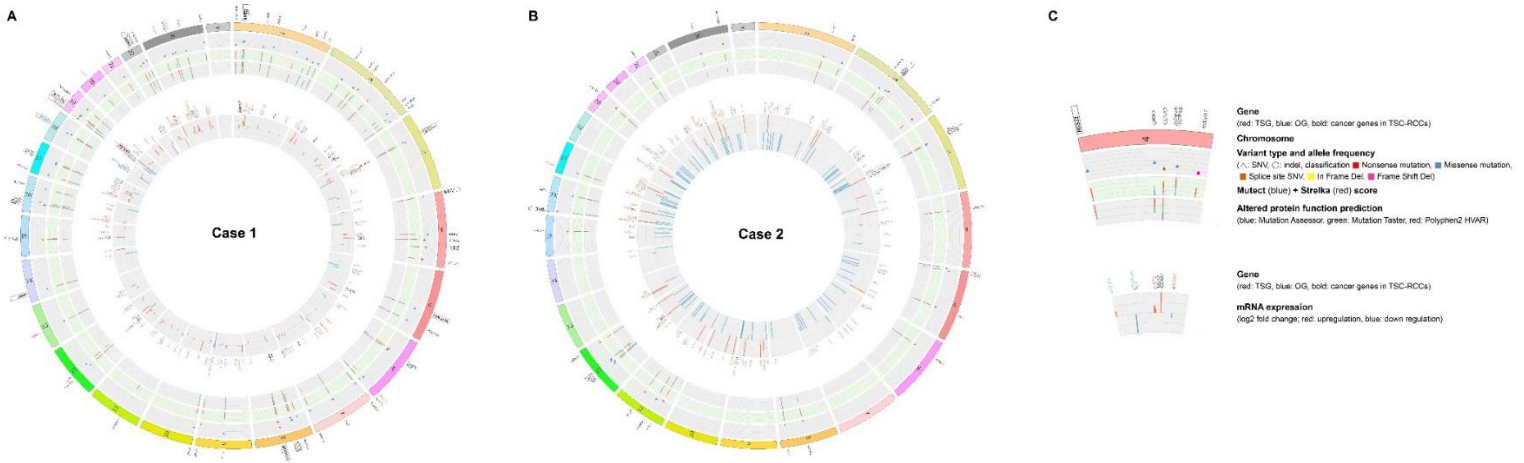

Figure 6. Somatic mutational spectrum of cancer-related genes in TSC-RCC cases. (A) TSC-RCC Case 1, (B) TSC-RCC Case 2 and (C) Circos plot inset legend.

Table 5. Alterations in cancer-related genes in TSC-RCC Case 1

Score	Hugo Symbol	Variant Classification	Variant Type	Ref Allele	Tumor Allele	Mutation Assessor	Mutation Taster	Polyphen2 HVAR	Mutect	Strelka	VAF (%)
3	*AFF3*	Splice_Site	SNV	C	T	.	D	.	1	2	8.33
2	*AMBRA1*	In_Frame_Del	DEL	CCTGGG	-				0	2	9.68
2	*AMER1*	Missense	SNV	C	T	L	D	D	2	0	13.33
2	*ARID1B*	Missense	SNV	T	A	N	N	B	2	0	14.81
3	*ASXL1*	Missense	SNV	G	C	L	N	B	1	2	9.30
3	*BCL11A*	Missense	SNV	C	T	M	D	P;D;B	1	2	7.32
3	*BCOR*	Missense	SNV	G	A	L	D	D	1	2	16.67
2	*BRD3*	Missense	SNV	T	C	L	D	P;B	2	0	12
3	*BTK*	Missense	SNV	C	T	M	D	B;P	1	2	10.71
3	*CACNA1D*	Missense	SNV	G	A	M	D	P;D	1	2	30.77
3	*CCNA2*	Splice_Site	SNV	G	A	H	D	D	1	2	10.71
3	*CDC27*	Missense	SNV	A	C	L	D	B	1	2	14.29
3	*CHD8*	Missense	SNV	G	A	M	D	D|.	1	2	22.22
3	*COL2A1*	Missense	SNV	C	T	H	D	D	1	2	18.18
2	*COL4A4*	Missense	SNV	G	A	L	N	B	2	0	9.52
2	*CR1*	Nonsense	SNV	C	T	.	A	.	2	0	13.04
3	*CRISPLD1*	Nonsense	SNV	C	T	.	A	.	1	2	36.36
2	*DKK2*	Missense	SNV	C	A	L	D	D	2	0	25

Score	Hugo Symbol	Variant Classification	Variant Type	Ref Allele	Tumor Allele	Mutation Assessor	Mutation Taster	Polyphen2 HVAR	Mutect	Strelka	VAF (%)
3	*DST*	Nonsense	SNV	G	A	.	A	.	1	2	10.71
4	*ENAH*	Missense	SNV	C	T	M	D	B	2	2	8.74
3	*EPB41L4A*	Missense	SNV	G	A	M	D	D	1	2	28.57
3	*FGFR1*	Missense	SNV	C	T	N	D	P	1	2	20
4	*FH*	Missense	SNV	C	T	M	D	D	2	2	13.79
2	*FN1*	Missense	SNV	C	T	L	D	B;P	0	2	30.77
3	*G6PD*	Missense	SNV	G	A	.	N	B	1	2	30.77
3	*GLI1*	Missense	SNV	G	A	L	D	B	1	2	30
3	*GNA11*	Splice_Site	SNV	C	T	H	D	D	1	2	28.57
3	*GTPBP1*	Missense	SNV	C	T	L	D	P	1	2	26.67
3	*HGF*	Missense	SNV	C	T	M	D	B;D;P	1	2	12.20
3	*IKBKB*	Missense	SNV	G	A	M	D	P;D	1	2	20
4	*INPP4B*	Missense	SNV	C	T	L	N	B	2	2	17.65
4	*INPP4B*	Missense	SNV	G	T	N	N	B	2	2	17.65
3	*ITGA2B*	Nonsense	SNV	G	A	.	A	.	1	2	13.95
3	*KAT6A*	Missense	SNV	C	T	L	D	B	1	2	9.84
3	*KMT2C*	Missense	SNV	G	A	L	D	B	1	2	9.84
4	*LPHN2*	Missense	SNV	G	A	.|.	D	.|.	2	2	12
3	*MAPK12*	Missense	SNV	G	A	M	D	D	1	2	30.77
3	*MAZ*	Missense	SNV	C	T	L	D	P;D	1	2	33.33

Score	Hugo Symbol	Variant Classification	Variant Type	Ref Allele	Tumor Allele	Mutation Assessor	Mutation Taster	Polyphen2 HVAR	Mutect	Strelka	VAF (%)
4	*MED12*	Missense	SNV	G	A	M	D	P;D;B	2	2	15
3	*MLLT4*	Missense	SNV	G	A	N	D	D;P	1	2	8.96
3	*NKX3-1*	Missense	SNV	G	C	N	N	B	1	2	12.12
4	*NOTCH3*	Splice_Site	SNV	G	A				2	2	25
3	*PAX8*	Splice_Site	SNV	A	T	.	D	.	1	2	14.81
3	*PBRM1*	Missense	SNV	C	T	L	D	D	1	2	21.05
3	*PDGFRB*	Missense	SNV	C	T	M	D	D	1	2	17.39
3	*PER2*	Missense	SNV	C	T	M	D	D	1	2	22.22
3	*PEX2*	Nonsense	SNV	G	A	.	D	.	1	2	13.16
2	*PFKP*	Missense	SNV	G	A	M	D	P|B	0	2	30.77
4	*PKHD1*	Missense	SNV	G	A	M	N	B	2	2	15.79
2	*PLA2G4E*	In_Frame_Del	DEL	GAGAACTGTCAG	-				0	2	6.52
4	*PLCB2*	Missense	SNV	A	T	N	D	B	2	2	10
3	*PLEKHG5*	Missense	SNV	G	A	M	D	P;D	1	2	11.11
2	*POLR2A*	Missense	SNV	G	A	M	D	D	0	2	28.57
3	*PRPF40A*	Missense	SNV	C	T	M	D	B;D	1	2	7.04
4	*PTPRU*	Missense	SNV	G	A	M	D	P	2	2	27.27
3	*RASGRP4*	Missense	SNV	C	T	M	D	D	1	2	20
4	*RBBP6*	Missense	SNV	C	T	L	D	D	2	2	11.76

Score	Hugo Symbol	Variant Classification	Variant Type	Ref Allele	Tumor Allele	Mutation Assessor	Mutation Taster	Polyphen2 HVAR	Mutect	Strelka	VAF (%)
3	*RBBP6*	Nonsense	SNV	C	T	.	A	.	1	2	15.79
3	*RBM15*	Missense	SNV	G	A	M	D	D	1	2	18.18
3	*RGS12*	Missense	SNV	C	T	L	D	P	1	2	22.22
3	*RLTPR*	Missense	SNV	G	A	N	D	D	1	2	21.05
3	*SETBP1*	Missense	SNV	G	A	L	D	D	2	1	12
3	*SETBP1*	Missense	SNV	G	A	L	D	D	1	2	30.77
3	*SMARCA4*	Missense	SNV	G	A	N	D	B;P	1	2	26.67
4	*STMN1*	Missense	SNV	C	T	M	D	D;P	2	2	25
3	*TIAM1*	Missense	SNV	G	A	N	D	B	1	2	19.05
3	*TJP2*	Missense	SNV	C	T	M	D	D;B	1	2	40
2	*TNN*	Missense	SNV	C	T	M	D	B	0	2	23.53
4	*TNRC18*	Missense	SNV	G	C	N	N	B	2	2	12.5
2	*WDR17*	Frame_Shift_Del	DEL	TGCTGGC	-				0	2	5.77
3	*ZC3H13*	Missense	SNV	C	T	.	D	D	1	2	5.56
3	*ZNRF3*	Missense	SNV	G	A	M	D	D	1	2	21.05

Abbreviations: A, disease causing automatic; B, benign; D (Mutation Taster), disease causing; D (Polyphen2 HVAR), probably damaging); H, high; L, low; M, medium; N, neutral; VAF, variant allele frequency

Table 6. Alterations in cancer-related genes in TSC-RCC Case 2

Score	Hugo Symbol	Variant Classification	Variant Type	Ref Allele	Tumor Allele	Mutation Assessor	Mutation Taster	Polyphen2 HVAR	Mutect	Strelka	VAF (%)
3	*ADCY2*	Missense	SNV	G	A	N	D	B	1	2	18.18
3	*AMBRA1*	Missense	SNV	C	T	L	D	D	2	1	15.79
3	*ANO3*	Nonsense	SNV	T	A	.	A	.	1	2	6.74
3	*APC*	Missense	SNV	G	A	L	D	D	1	2	7.48
3	*ARHGEF6*	Splice_Site	SNV	A	G	N	D	B	1	2	25
3	*CACNA2D3*	Splice_Site	SNV	G	A	M	D	D	2	1	11.11
3	*CALM3*	Nonsense	SNV	C	T	.	A	.	1	2	9.26
2	*COL4A3*	Frame_Shift_Del	DEL	ATCCC TGG	-				0	2	13.79
3	*DLG2*	Nonsense	SNV	G	A	.	D	.	1	2	17.39
3	*ERC2*	Missense	SNV	C	T	L	D	D	1	2	5.11
3	*FOXP4*	Missense	SNV	C	T	M	D	D	1	2	5.56
3	*GLI1*	Missense	SNV	C	T	M	D	P	1	2	5.26
3	*GRXCR1*	Missense	SNV	C	T	L	D	D	1	2	8.45
3	*HERC1*	Missense	SNV	C	T	N	D	D	1	2	8.33
4	*IWS1*	Splice_Site	SNV	T	C	N	D	B	2	2	21.21
3	*LAMC1*	Missense	SNV	G	A	M	D	P	1	2	6.90

Score	Hugo Symbol	Variant Classification	Variant Type	Ref Allele	Tumor Allele	Mutation Assessor	MutationTaster	Polyphen2 HVAR	Mutect	Strelka	VAF (%)
3	*MAP4K4*	Missense	SNV	C	T	M	D	D	1	2	6
3	*MTR*	Missense	SNV	C	A	M	N	B	1	2	10.81
4	*MYC*	Missense	SNV	C	T	M	D	D	2	2	7.27
3	*NCOR1*	Missense	SNV	G	A	L	D	D;B	1	2	10.64
3	*NKD1*	Missense	SNV	G	A	M	D	D	1	2	5.04
3	*RALB*	Missense	SNV	G	A	N	D	B	1	2	17.39
4	*RAP1B*	Missense	SNV	G	A	L	D	B;P	2	2	12.73
2	*SBNO1*	Nonsense	SNV	G	A	.	A	.	0	2	8.62
3	*SP1*	Missense	SNV	C	T	M	D	D	1	2	12.12
2	*TAF1*	Missense	SNV	G	A	L	D	B	2	0	8.57
4	*TIAM1*	Missense	SNV	C	T	M	D	D	2	2	7.27
3	*TRIP13*	Missense	SNV	C	T	M	D	D	1	2	7.23
4	*TSC2*	Nonsense	SNV	C	T	.	A	.	2	2	58.33
3	*WNT5A*	Missense	SNV	G	A	N	D	B	1	2	7.06
2	*XPOT*	Missense	SNV	G	C	L	D	B	2	0	17.39
3	*ZFHX4*	Missense	SNV	G	A	L	D	B	1	2	5.26

Abbreviations: A, disease causing automatic; B, benign; D (Mutation Taster), disease causing; D (Polyphen2 HVAR), probably damaging); H, high; L, low; M, medium; N, neutral; VAF, variant allele frequency

Genetic alterations of cancer genes in TSC-RCC cases

To assess the pathogenic basis of each TSC-RCC case, we analysed alterations of cancer genes (Table 7 and Figure 7). In Case 1, 12 cancer genes were identified. These included *CHD8*, *CRISPLD1*, *EPB41L4A*, *GNA11*, *NOTCH3*, *PBRM1*, *PTPRU*, *RGS12*, *SETBP1*, *SMARCA4*, *STMN1* and *ZNRF3*. All mutations were classified as SNVs and there were 9 missense mutations, 1 nonsense mutation and 2 splice site SNVs. In Case 2, we identified 2 altered cancer genes. These included *IWS1* and *TSC2*. All mutations were classified as SNVs, and there were 1 nonsense mutation and 1 splice site SNVs. Above genes were validated by Sanger sequencing. However, cancer genes from Case 1 were not available for Sanger sequencing due to low tumour purity and tissue quality (inflammation and abscess).

Table 7. Somatic mutations of cancer genes in TSC-RCC patients

Case	Score	Gene	Driver	Role	Variant Classification	Variant Type	Ref	Alt	cDNA Change	Protein Change	VAF (%)	Validation
1	3	*CHD8*	.	.	Missense	SNV	G	A	c.2368C>T	p.R790C	22.22	+[a]
	3	*CRISPLD1*	.	.	Nonsense	SNV	C	T	c.1363C>T	p.R455*	36.36	NA
	3	*EPB41L4A*	.	.	Missense	SNV	G	A	c.1618C>T	p.R540C	28.57	NA
	3	*GNA11*	+	OG	Splice Site	SNV	C	T	c.604C>T	p.R202W	28.57	+[a]
	4	*NOTCH3*	.	.	Splice Site	SNV	G	A	c.1194C>T	p.G398G	25	+[a]
	3	*PBRM1*	+	TSG	Missense	SNV	C	T	c.49G>A	p.G17R	21.05	+[a]
	4	*PTPRU*	.	.	Missense	SNV	G	A	c.1412G>A	p.R471H	27.27	+[a]
	3	*RGS12*	.	.	Missense	SNV	C	T	c.4073C>T	p.P1358L	22.22	NA
	3	*SETBP1*	+	OG	Missense	SNV	G	A	c.2572G>A	p.E858K	30.77	+[a]
	3	*SMARCA4*	+	TSG	Missense	SNV	G	A	c.3067G>A	p.E1023K	26.67	+[a]
	4	*STMN1*	.	.	Missense	SNV	C	T	c.235G>A	p.E79K	25	+[a]
	3	*ZNRF3*	.	.	Missense	SNV	G	A	c.1361G>A	p.R454H	21.05	+[a]
2	4	*IWS1*	.	.	Splice Site	SNV	T	C	c.2048A>G	p.N683S	21.21	+[b]
	4	*TSC2*	.	.	Nonsense	SNV	C	T	c.1372C>T	p.R458*	58.33	+[b]

[a]Validation was performed with droplet digital PCR

[b]Validation was performed with Sanger sequencing

Abbreviations: NA, not available; OG, oncogene; TSG, tumor suppressor gene; VAF, variant allele frequency

Score: Mutect score + Strelka score

Case 1 Tumor tissue

CHD8 c.2368C>T p.R790C

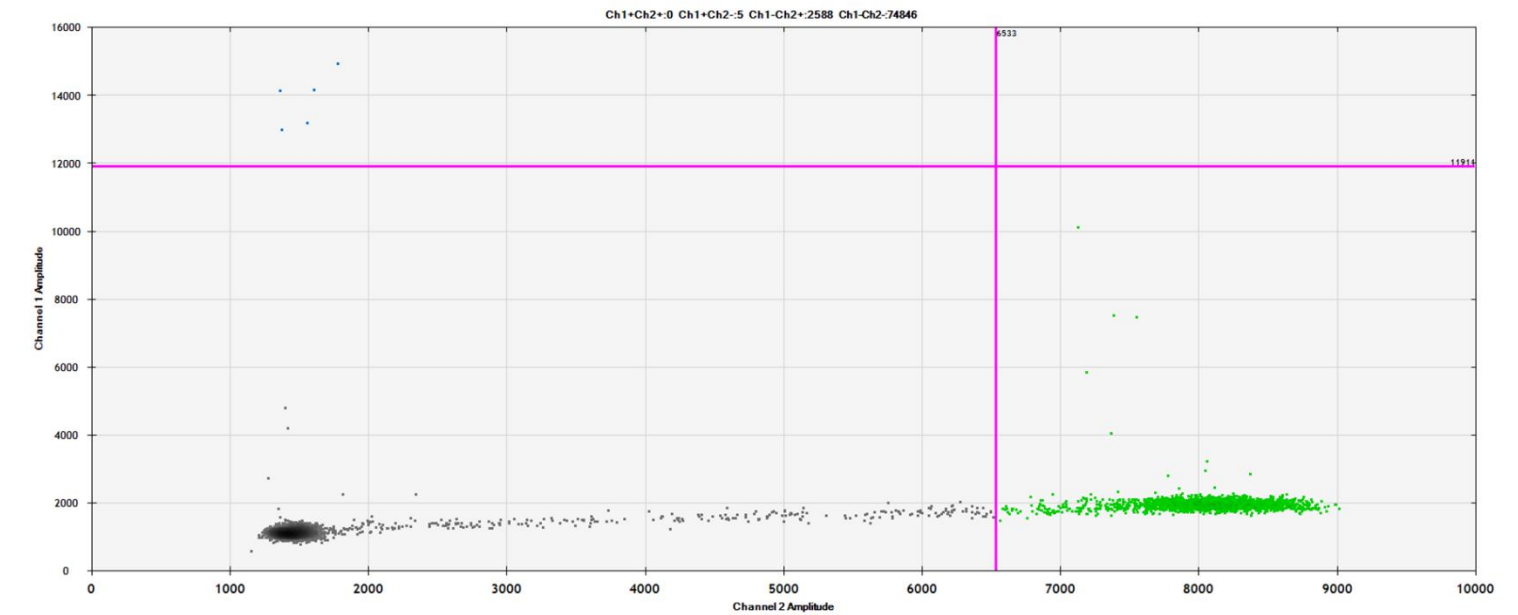

(2D plot)

Figure 7. Validation of cancer genes in TSC-RCC cases

Case 1 Tumor tissue

GNA11 c.604C>T p.R202W

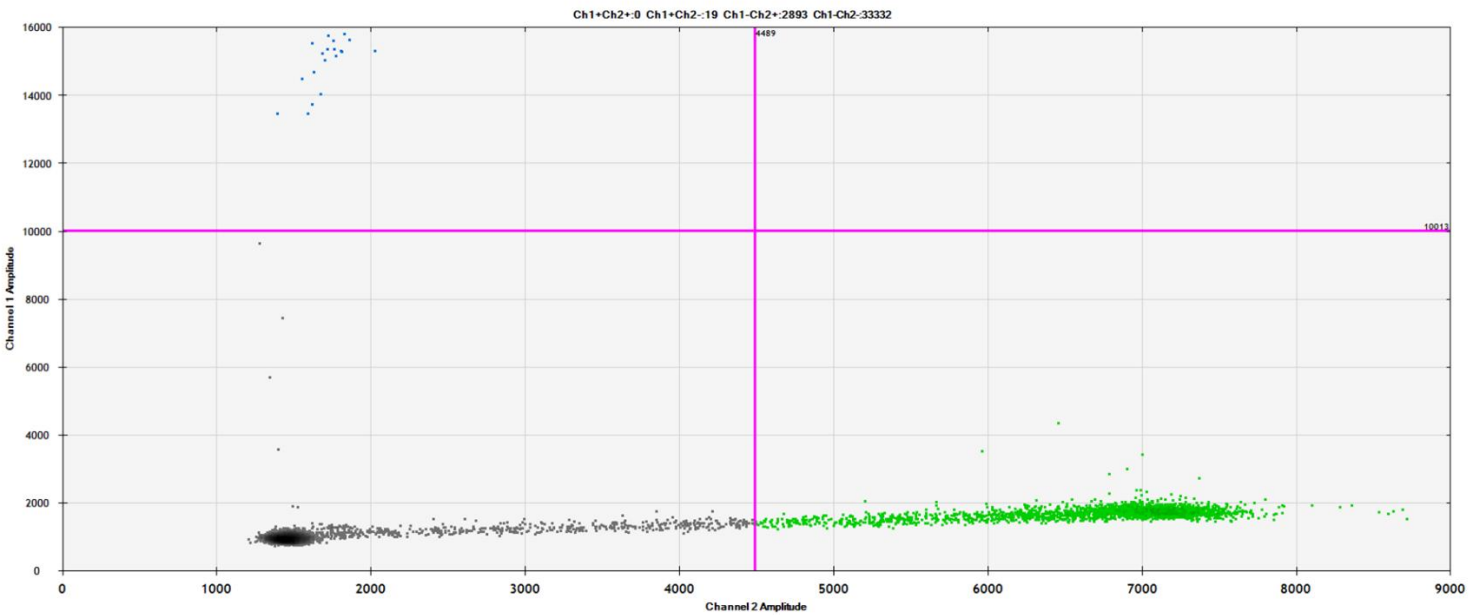

(2D plot)

Figure 7. Validation of cancer genes in TSC-RCC cases

Case 1 Tumor tissue

NOTCH3 c.1194C>T p.G398G

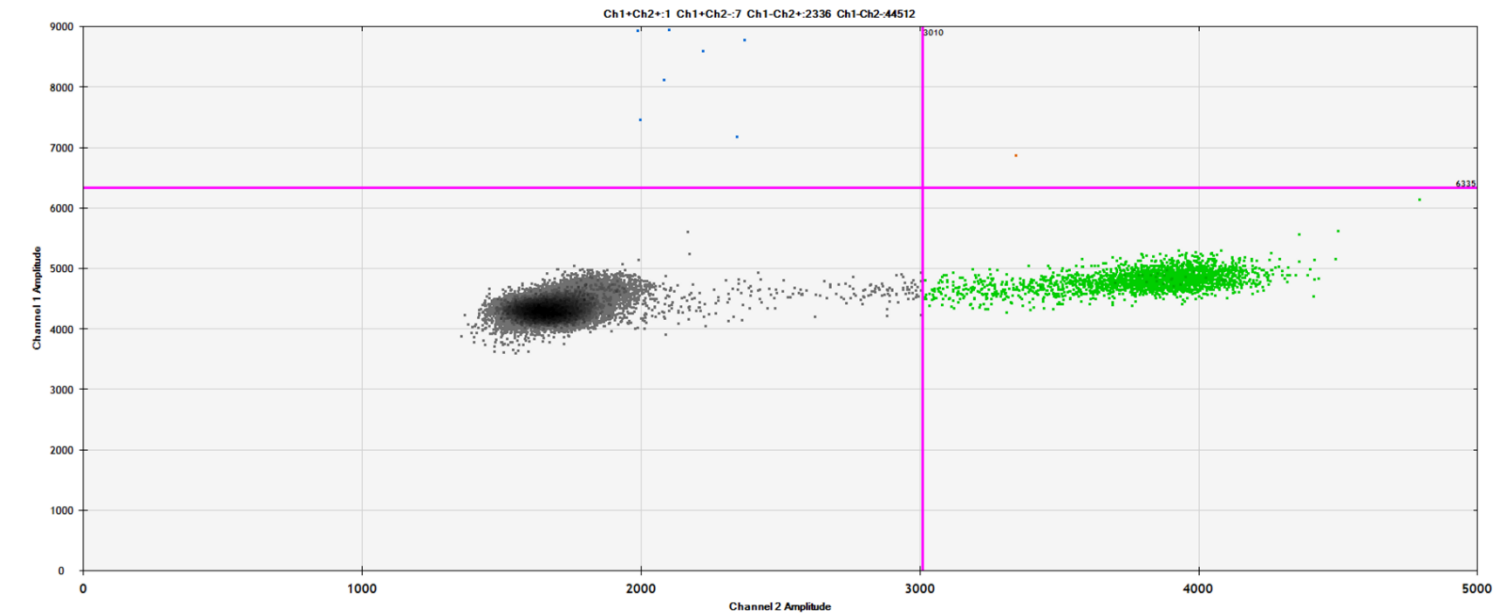

(2D plot)

Figure 7. Validation of cancer genes in TSC-RCC cases

Case 1 Tumor tissue

PBRM1 c.49G>A p.G17R

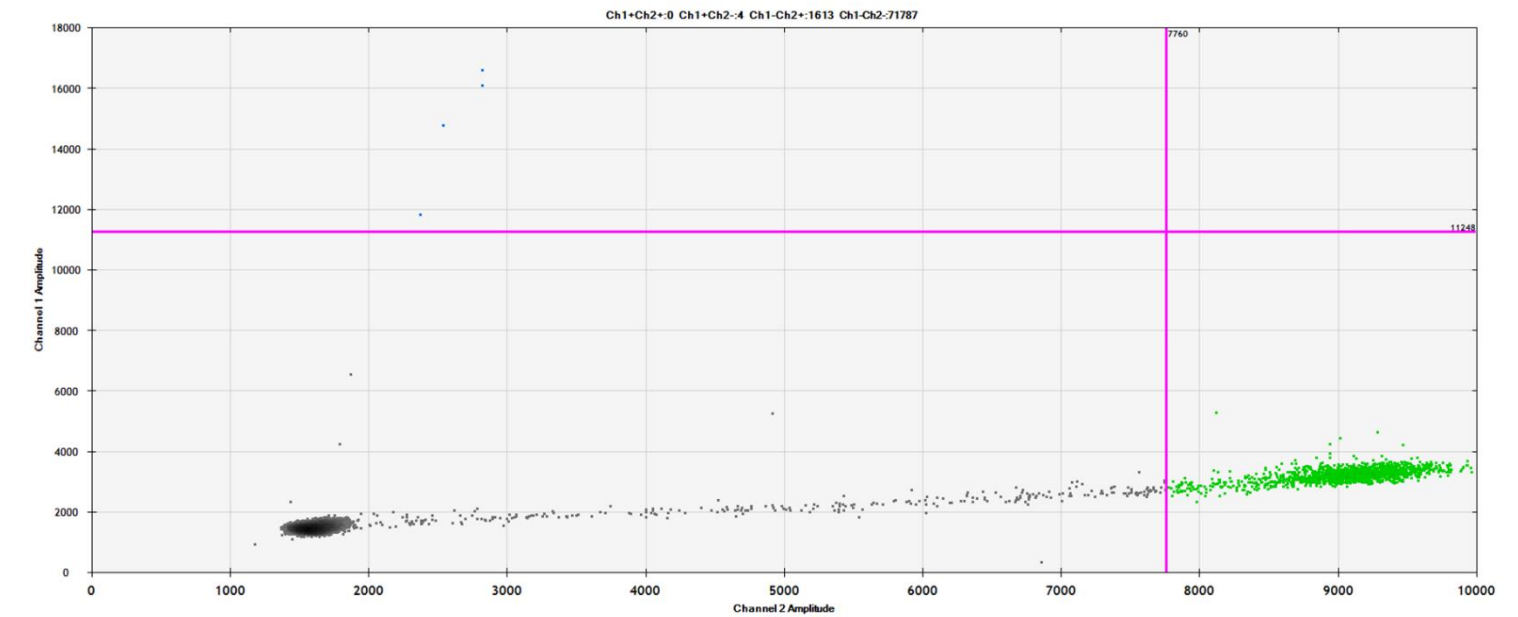

(2D plot)

Figure 7. Validation of cancer genes in TSC-RCC cases

Case 1 Tumor tissue

PTPRU c.1412G>A p.R471H

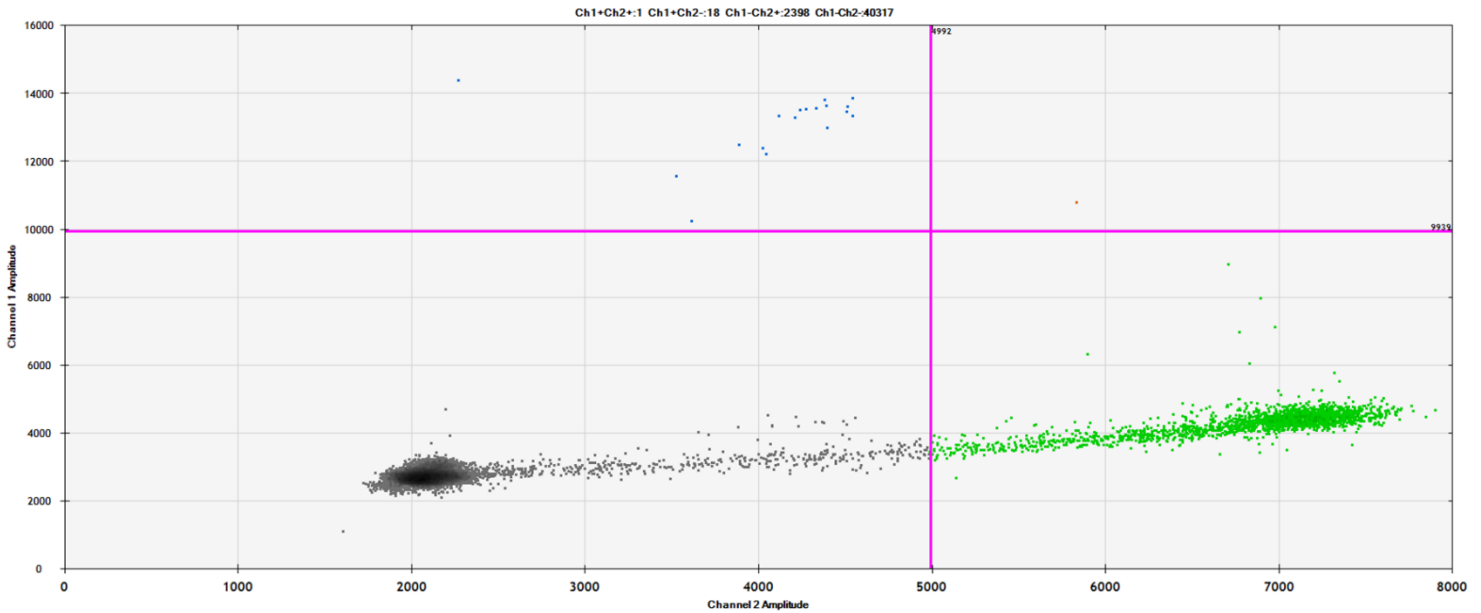

(2D plot)

Figure 7. Validation of cancer genes in TSC-RCC cases

Case 1 Tumor tissue

SETBP1 c.2572G>A p.E858K

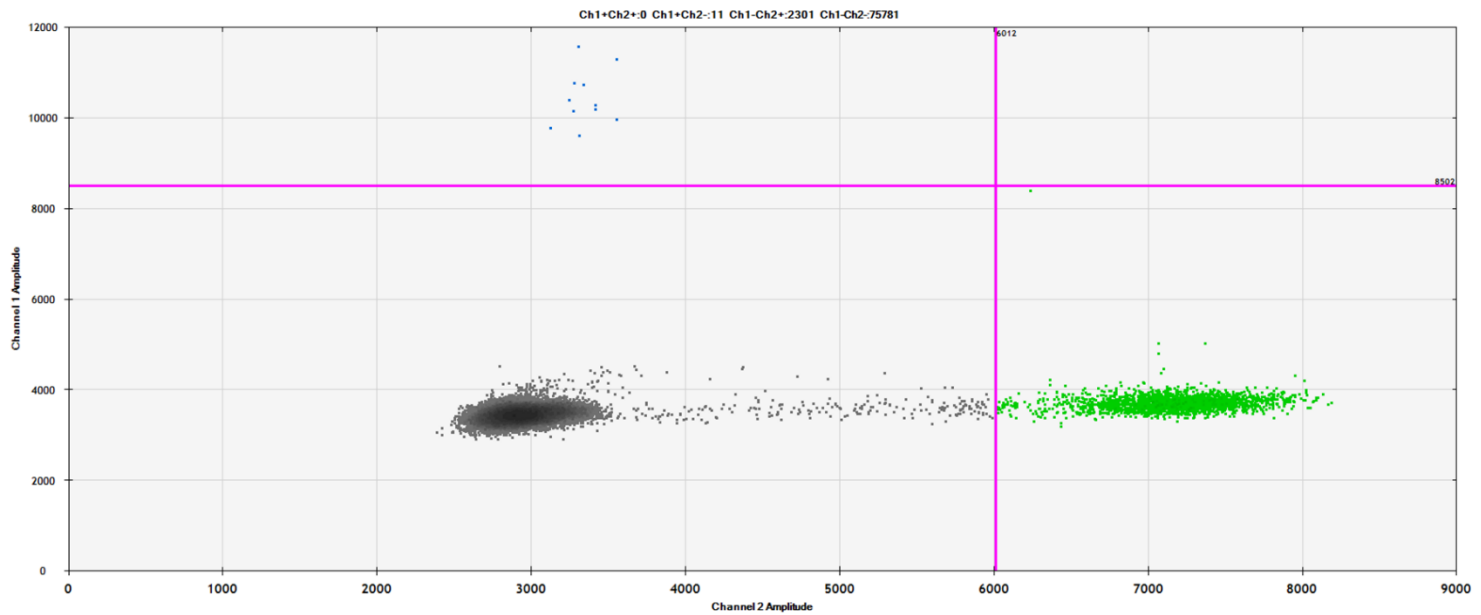

(2D plot)

Figure 7. Validation of cancer genes in TSC-RCC cases

Case 1 Tumor tissue

SMARCA4 c.3067G>A p.E1023K

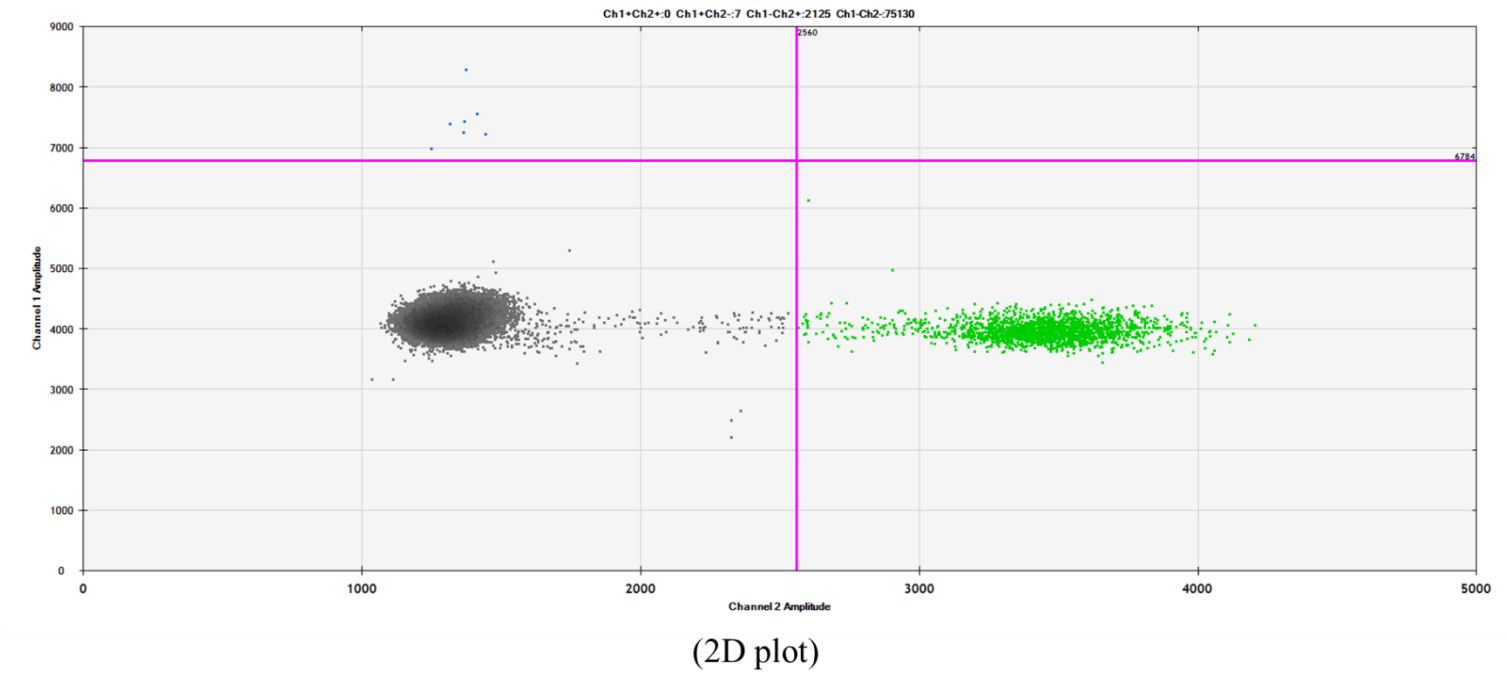

(2D plot)

Figure 7. Validation of cancer genes in TSC-RCC cases

Case 1 Tumor tissue

STMN1 c.235G>A p.E79K

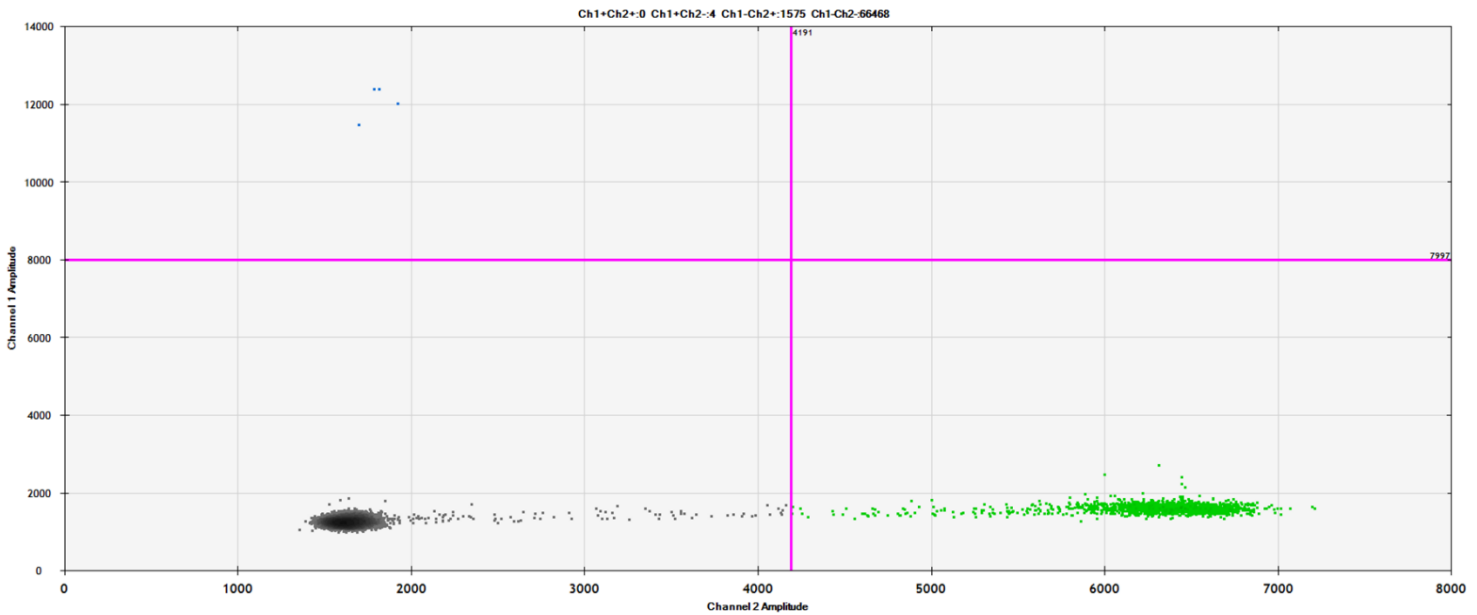

(2D plot)

Figure 7. Validation of cancer genes in TSC-RCC cases

Case 1 Tumor tissue

ZNRF3 c.1361G>A p.R454H

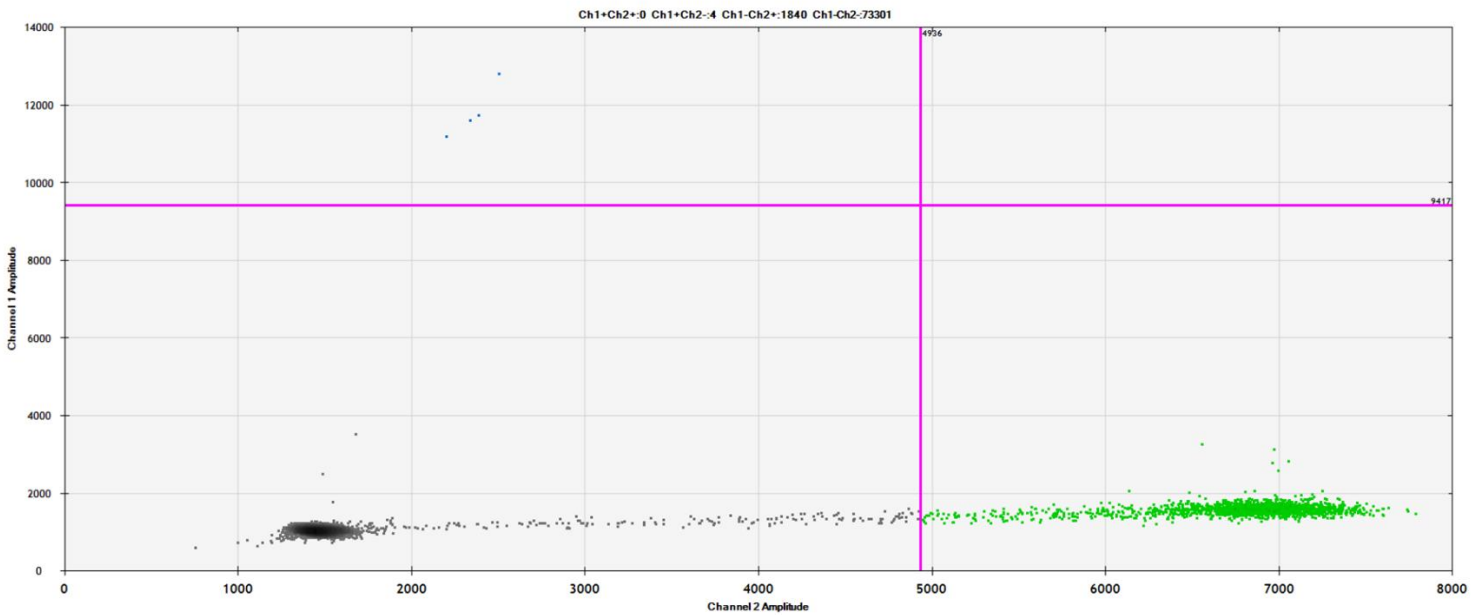

(2D plot)

Figure 7. Validation of cancer genes in TSC-RCC cases

Case 2 Tumor tissue

IWS1 c.2048A>G p.N683S

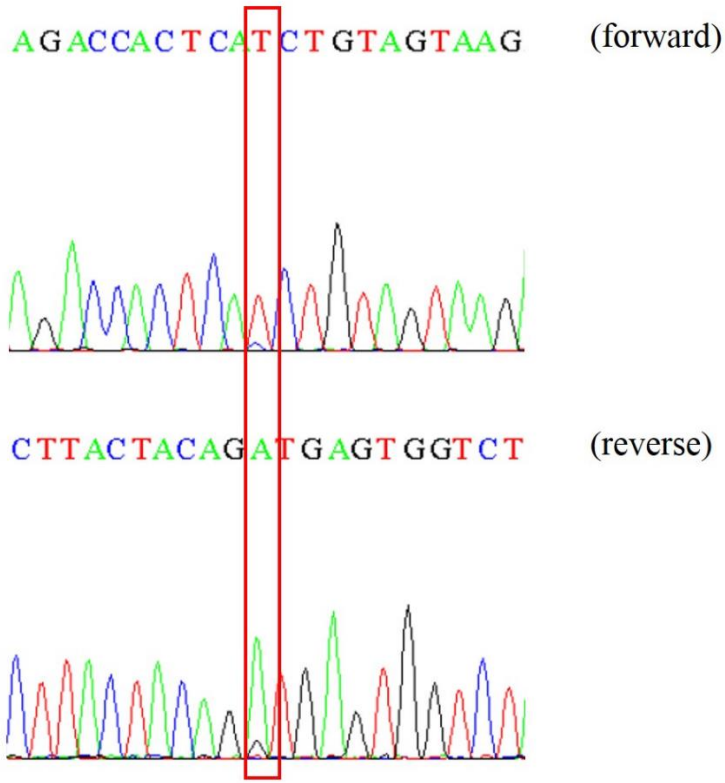

Figure 7. Validation of cancer genes in TSC-RCC cases

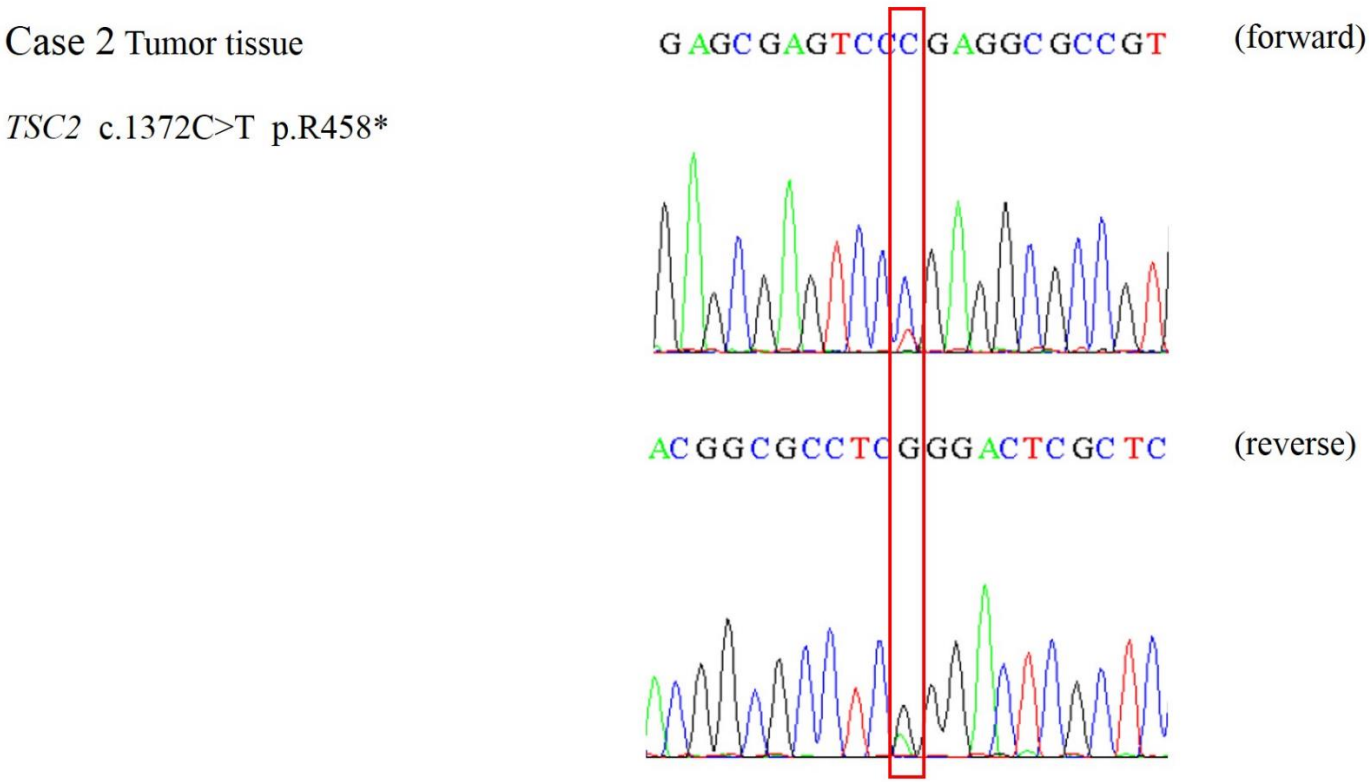

Figure 7. Validation of cancer genes in TSC-RCC cases

Copy number variation and loss of heterozygosity in TSC-RCC cases

In both TSC-RCCs, there were no megabase-scale amplification or deletion. Also, LOH including chromosome 16 (*TSC2*, chr.16p13.3) was not found in both TSC-RCCs (Figure 8 and 9).

(A)

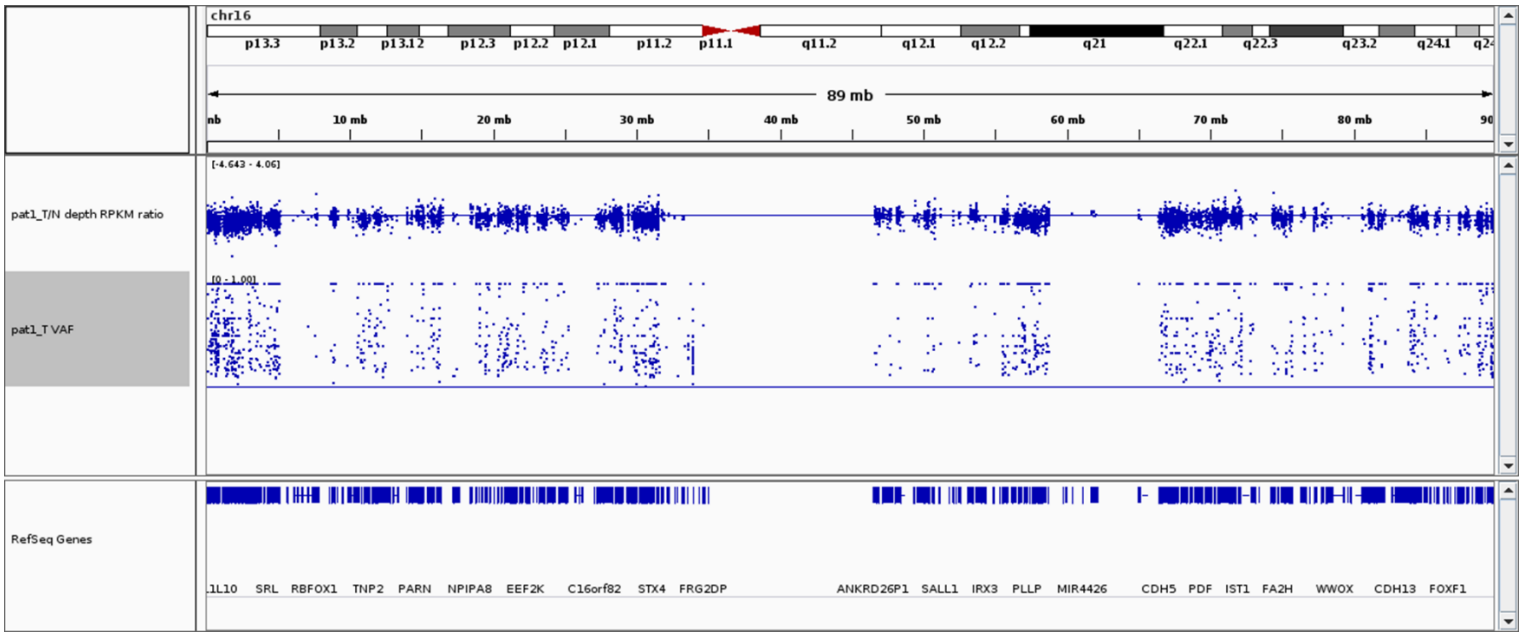

Figure 8. Copy number variation and loss of heterozygosity analysis in TSC-RCC Case 1. (A) RPKM

(B)

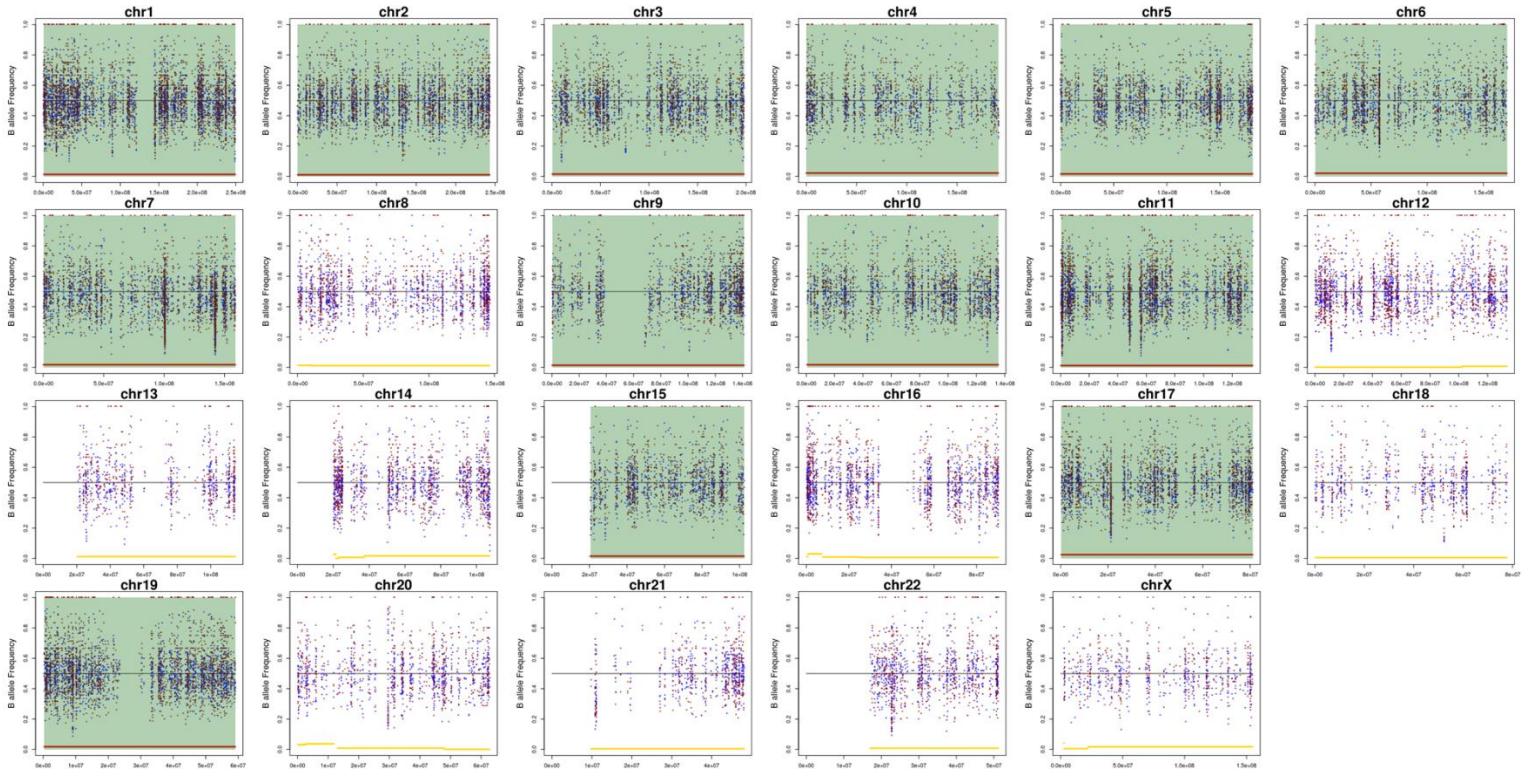

Figure 8. Copy number variation and loss of heterozygosity analysis in TSC-RCC Case 1. (B) LOH plot

(C)

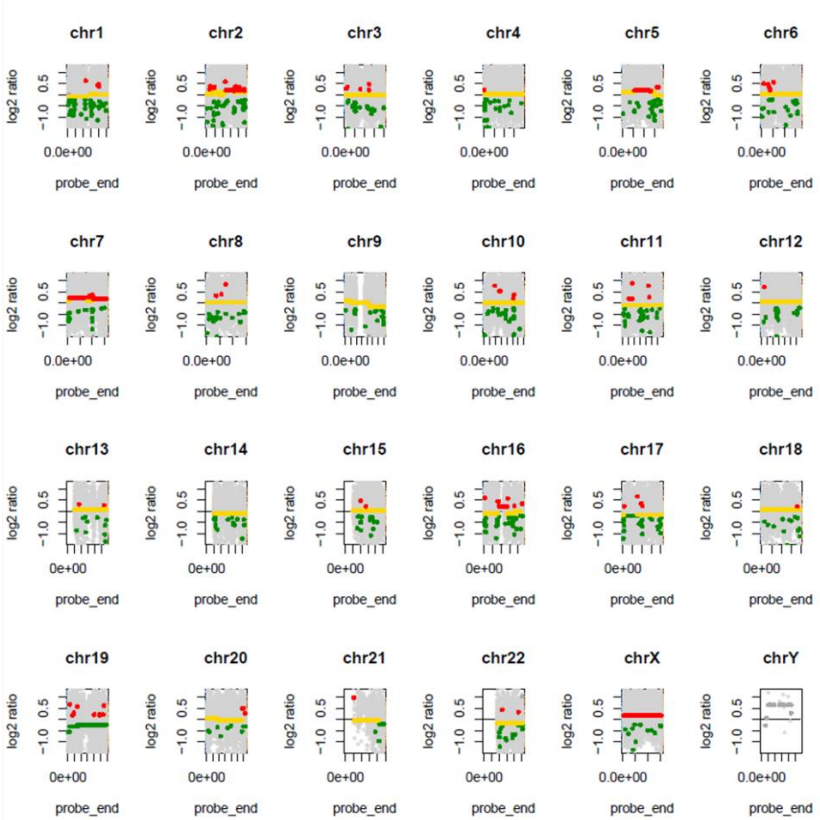

Figure 8. Copy number variation and loss of heterozygosity analysis in TSC-RCC Case 1. (C) CNV plot

(A)

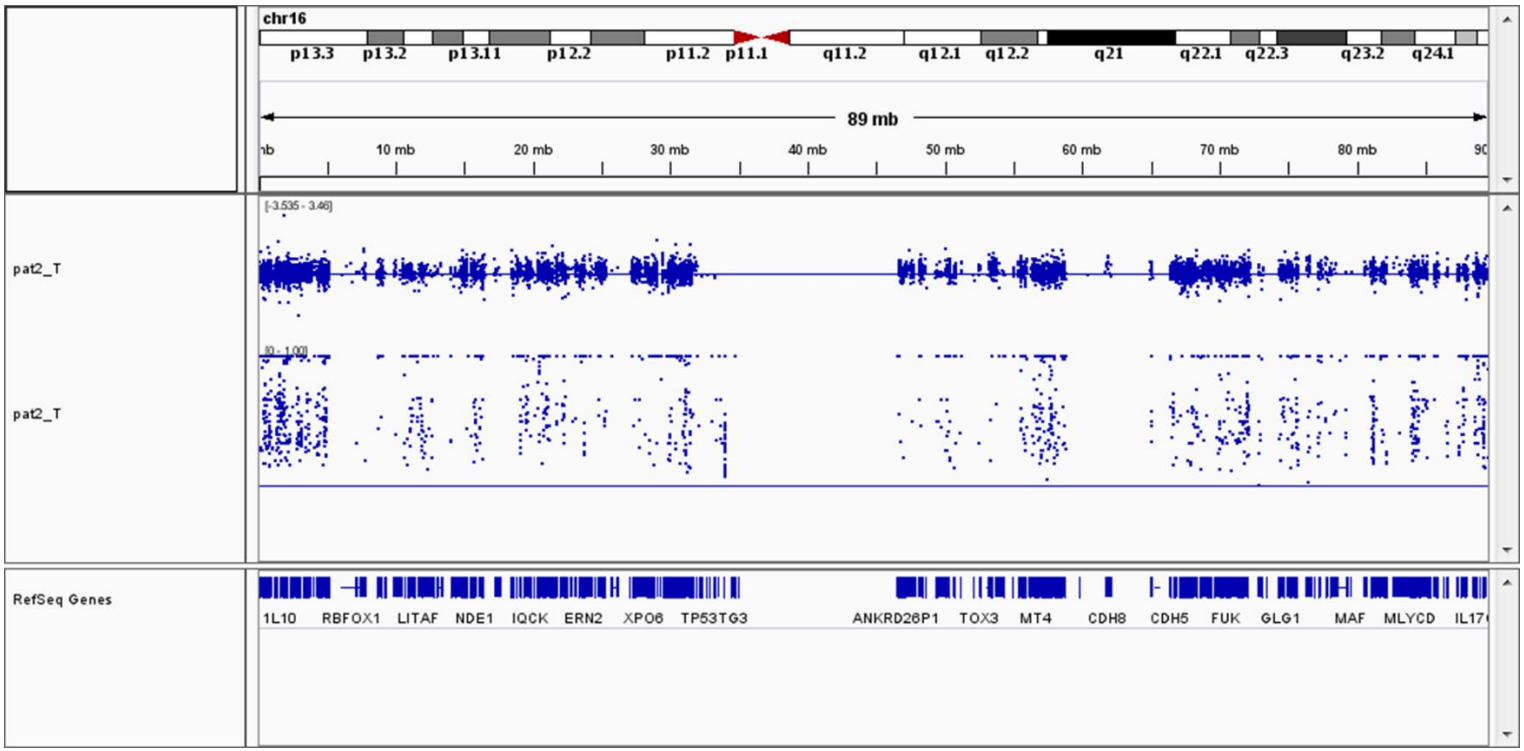

Figure 9. Copy number variation and loss of heterozygosity analysis in TSC-RCC Case 2. (A) RPKM

(B)

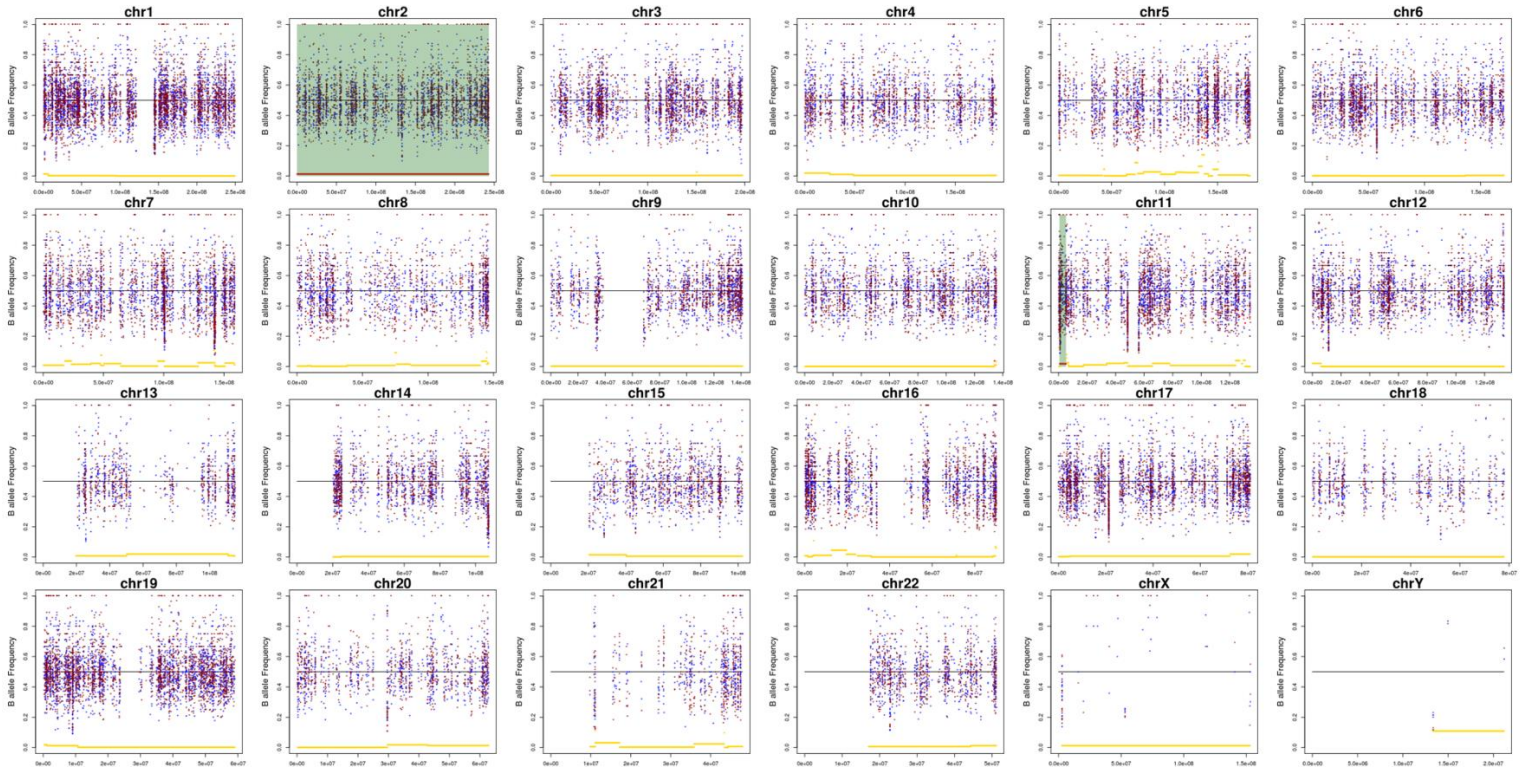

Figure 9. Copy number variation and loss of heterozygosity analysis in TSC-RCC Case 2. (B) LOH plot

(C)

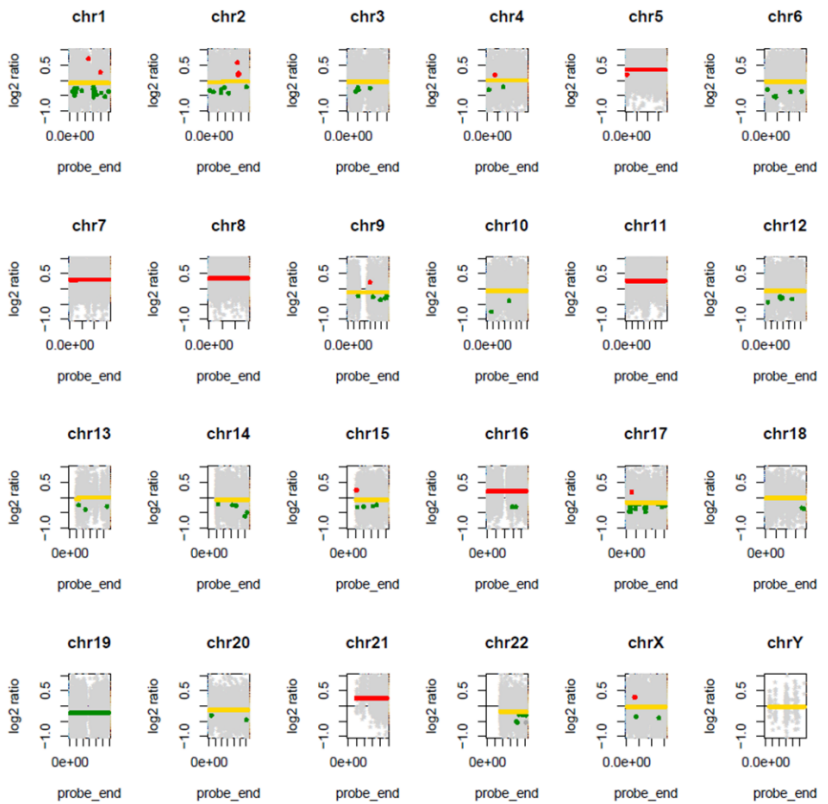

Figure 9. Copy number variation and loss of heterozygosity analysis in TSC-RCC Case 2. (C) CNV plot

Putative pathogenic pathways in TSC-RCC cases

We assess putative pathogenic pathways for each TSC-RCC case (Figure 10 and Table 8). In Case 1, putative pathogenic pathways were chromatin remodelling pathway (*CHD8*, *PBRM1* and *SMARCA4*), G protein-coupled receptor (GPCR) pathway (*GNA11* and *RGS12*), Notch signalling pathway (*NOTCH3*), Wnt/β-catenin pathway (*PTPRU* and *ZNRF3*), PP2A pathway (*SETBP1*) and microtubule dynamics pathway (*STMN1*). In Case 2, putative pathogenic pathways were mRNA processing (*IWS1*) and PI3K/AKT/mTOR pathway (*TSC2*).

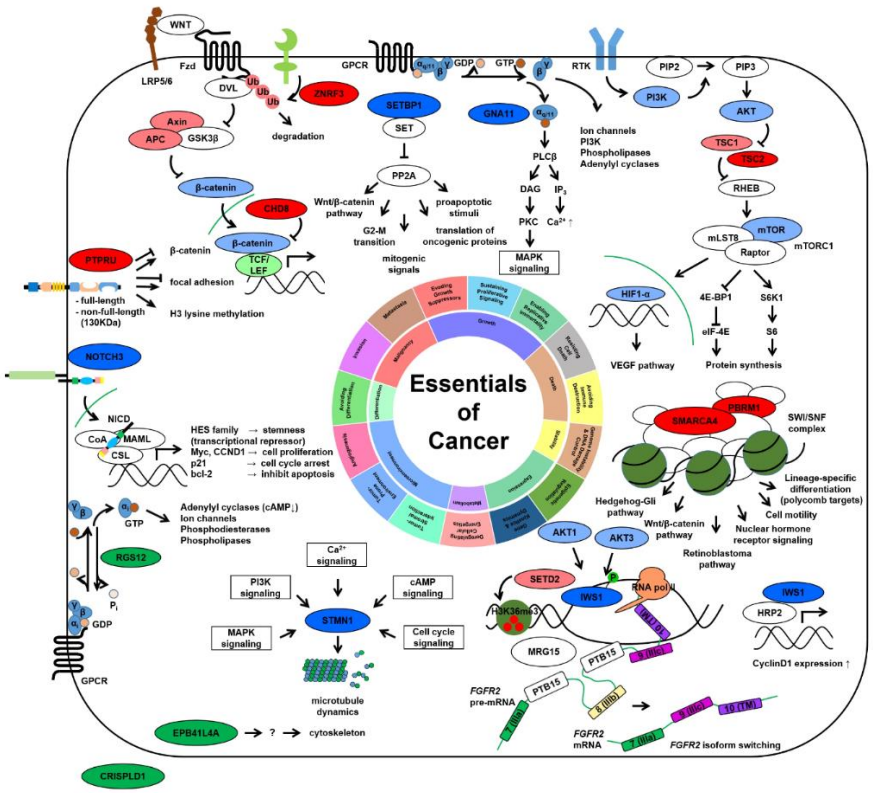

Figure 10. Putative pathogenic pathways in TSC-RCC cases (red: tumour suppressor gene; blue: oncogene; bold: cancer genes in TSC-RCCs)

Table 8. Putative pathogenic pathways in TSC-RCC patients

Case	Gene	Driver	Role	Pathway	Biologic function	Tumors
1	*CHD8*	-	TSG > OG	chromatin remodeling	cell survival; cell proliferation	hematopoietic malignancy, gastric cancer, colorectal cancer, prostate cancer, breast cancer
	CRISPLD1	-	.	.	.	.
	EPB41L4A	-	.	.	.	laterally spreading tumor (colorectum), non-medullary thyroid cancer
	GNA11	+	OG	GPCR pathway	cell proliferation; cell survival; invasion; apoptosis; differentiation; migration	melanoma, mesothelioma, endometrial cancer, esophageal cancer, breast cancer, ovarian (mucinous) cancer
	NOTCH3	-	OG > TSG	Notch signaling pathway	stem-like property; differentiation; cell proliferation; cell motility; invasiveness; metastasis; cell adhesion; epithelial mesenchymal transition; apoptosis; cellular senescence	breast cancer, T-cell acute lymphoblastic leukemia, B-cell acute lymphoblastic leukemia, ovarian cancer, lung cancer, oral squamous cell carcinoma, pancreatic ductal adenocarcinoma, colorectal carcinoma, skin cancer, melanoma, hepatocellular carcinoma, thyroid cancer, cholangiocarcinoma, renal cell carcinoma, gastric cancer, esophageal cancer, laryngeal cancer, glioblastoma, endometrial cancer, EBV-associated nasopharyngeal cancer, cervical squamous cell carcinoma, chondrosarcoma, Ewing sarcoma family of tumors
	PBRM1	+	TSG	chromatin remodeling	cell cycle progression; invasiveness; stemness; differentiation	clear cell renal cell carcinoma, breast cancer, bladder cancer, cholangiocarcinoma, mesothelioma, gallbladder cancer, prostate cancer, thymic carcinoma, gastric cancer
	PTPRU	-	TSG > OG	Wnt/β-catenin pathway	cell proliferation, focal adhesion; cell motility; invasiveness	non-small cell lung carcinoma, small cell lung carcinoma, colon cancer, endometrial cancer, stomach cancer, glioma, melanoma
	RGS12	-	.	GPCR pathway	.	.

Case	Gene	Driver	Role	Pathway	Biologic function	Tumors
	SETBP1	+	OG	PP2A pathway	cell proliferation; apoptosis; cell survival; cell migration; differentiation	hematologic malignancy (leukemia, therapy-related myeloid neoplasms, therapy-related acute lymphoblastic leukemia, atypical chronic myeloid leukemia)
	SMARCA4	+	TSG	chromatin remodeling	cell cycle progression; invasiveness; stemness; differentiation	small cell carcinoma of the ovary, hypercalcemic type, non-small cell lung carcinoma, ampullary and pancreatic ductal adenocarcinoma, endometrioid adenocarcinoma, colorectal cancer, rhabdoid tumor, thoracic sarcoma, Wilm tumor, neuroendocrine carcinoma, Burkitt lymphoma, oligodendroglioma, gastric cancer, thymic carcinoma, clear cell renal cell carcinoma, mantle cell lymphoma, cervical cancer, medulloblastoma
	STMN1	-	OG	microtubule dynamics	cell cycle progression; invasiveness; metastasis	gastric cancer, breast cancer, non-small cell lung carcinoma, gallbladder cancer, cutaneous squamous cell carcinoma, oral squamous cell carcinoma, colorectal cancer, osteosarcoma, melanoma, bladder cancer, ovarian cancer, high grade pelvic serous carcinoma, prostate cancer, hepatocellular carcinoma, endometrial cancer, acute myelogenous leukemia, lymphoma, neuroblastoma, mesothelioma, HPV-positive oropharyngeal carcinoma, hypopharyngeal squamous cell carcinoma, nasopharyngeal carcinoma, laryngeal squamous cell carcinoma, small cell lung carcinoma, myelodysplastic syndrome, glioma
	ZNRF3	-	TSG	Wnt/β-catenin pathway	cell proliferation; apoptosis; cell cycle progression; invasiveness	colorectal cancer, gastric cancer, lung cancer, papillary thyroid carcinoma, osteosarcoma, adrenocortical carcinoma

Case	Gene	Driver	Role	Pathway	Biologic function	Tumors
2	*IWS1*	-	OG (> TSG)	mRNA processing	tumor growth; migration; invasiveness	lung cancer, colon cancer, hepatocellular carcinoma
	TSC2	-	TSG	PI3K/AKT/ mTOR pathway	cell proliferation; cell growth; metabolism; angiogenesis; cell survival; cell mobilization	lymphangioleiomyomatosis, renal angiomyolipojma, head and neck squamous cell carcinoma, renal cell carcinoma, hamartoma, cortical tuber, subependymal giant cell astrocytoma, angiofibroma

Abbreviations: OG, oncogene; TSG, tumor suppressor gene

Genetic alterations in RCC-related genes

Several RCC-related gene alterations were identified (Figure 11 and table 9 and 10). In Case 1, these included *AHNAK2* (CCRCC), *CUBN* and *SMARCA4* (PRCC), *AFF3*, *CDC27*, *DSPP*, *PRODH*, *YLPM1* and *ZNF598* (ChRCC), *KMT2C* and *PBRM1* (CCRCC and PRCC) and *MUC2 and TTN* (CCRCC, PRCC and ChRCC). Additionally, *FH*, *KMT2C* and *PBRM1* genes were in common with unclassified RCC. In Case 2, only *TG* (ChRCC) was identified. Additionally, the *TSC2* gene was in common with unclassified RCC. The *USP34* (Case 1) and *NDE1* (Case 2) alterations in TSC-associated papillary RCC were found.

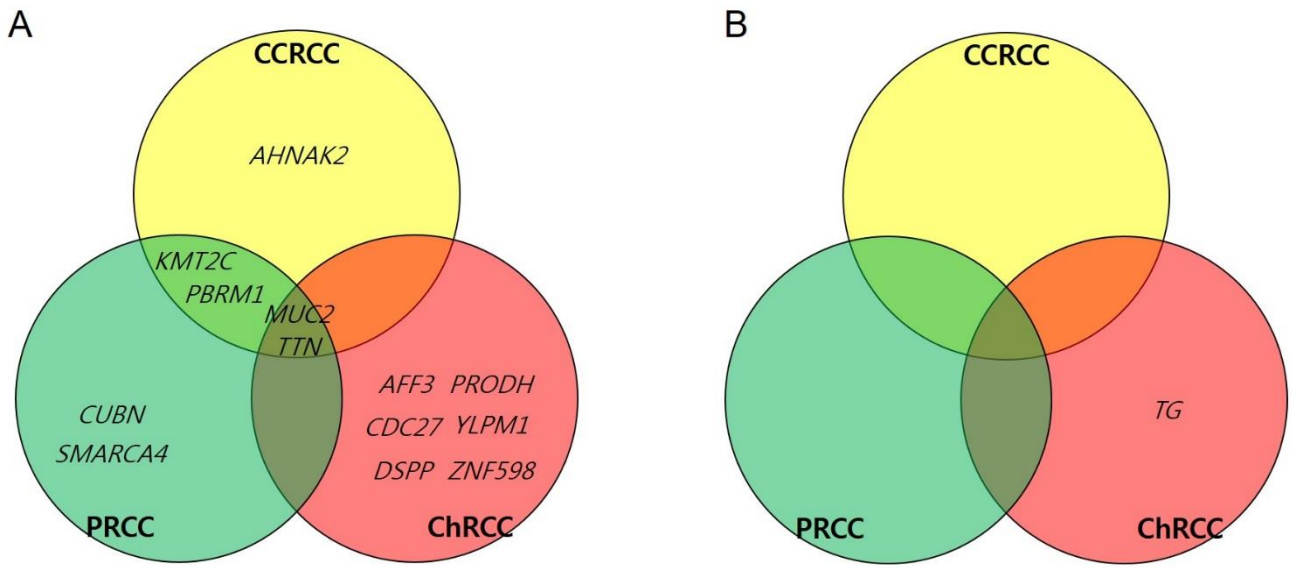

Figure 11. Altered genes in common with renal cell carcinoma (A) TSC-RCC Case 1 and (B) TSC-RCC Case 2.

Table 9. Frequency of genetic mutations in common RCC subtypes

Case	Gene	Frequency	RCC subtype
1	*AHNAK2*	4.01%	CCRCC
	CUBN	4.26%	PRCC
	SMARCA4	3.55%	PRCC
	AFF3	3.08%	ChRCC
	CDC27	3.08%	ChRCC
	DSPP	3.08%	ChRCC
	PRODH	3.08%	ChRCC
	TTN	18.50%	PRCC
		14.60%	CCRCC
		4.62%	ChRCC
	YLPM1	3.08%	ChRCC
	ZNF598	3.08%	ChRCC
	KMT2C	4.01%	CCRCC
		6.38%	PRCC
	PBRM1	36.08%	CCRCC
		3.90%	PRCC
	MUC2	3.07%	CCRCC
		3.90%	PRCC
		3.08%	ChRCC
2	*TG*	3.08%	ChRCC

Table 10. Frequently altered genes in common RCC subtypes

CCRCC				PRCC				ChRCC			
Gene	MutSig[a]	#Case	Freq[b]	Gene	MutSig[a]	#Case	Freq[b]	Gene	MutSig[a]	#Case	Freq[b]
VHL	3.62E-12	218	51.20	TTN		51	18.50	TP53	0	20	30.80
PBRM1	3.69E-12	153	35.90	MUC16		27	9.80	PTEN	3.62E-07	6	9.20
MUC4		90	21.10	MET		23	8.30	TTN		3	4.60
TTN		62	14.60	PKHD1		19	6.90	ICE1		3	4.60
SETD2	3.62E-12	55	12.90	KMT2C		19	6.90	KIAA1211		3	4.60
BAP1	1.55E-11	42	9.90	KIAA1109		19	6.90	ZFHX3		2	3.10
MUC16		34	8.00	KMT2D		18	6.50	ATM		2	3.10
KDM5C	6.54E-09	29	6.80	OBSCN		18	6.50	CACNA1A		2	3.10
MTOR	8.16E-06	23	5.40	SETD2		17	6.20	CACNA1B		2	3.10
PABPC1		19	4.50	FAT1		16	5.80	CASP5		2	3.10
HMCN1		18	4.20	MACF1		16	5.80	CDC27	3.03E-04	2	3.10
PTEN	2.88E-08	17	4.00	USH2A		15	5.40	CDKN1A	3.50E-02	2	3.10
USH2A		17	4.00	DNAH8		14	5.10	CLCN2		2	3.10
KMT2C		17	4.00	BAP1		14	5.10	CSF2RB		2	3.10

CCRCC				PRCC				ChRCC			
Gene	MutSig[a]	#Case	Freq[b]	Gene	MutSig[a]	#Case	Freq[b]	Gene	MutSig[a]	#Case	Freq[b]
AHNAK2		17	4.00	WDFY3		14	5.10	DSCAM		2	3.10
MAGEC1		16	3.80	CUBN		13	4.70	DSPP		2	3.10
DNAH9		15	3.50	HERC2		13	4.70	FLT4		2	3.10
SYNE1		15	3.50	HUWE1		13	4.70	MTOR		2	3.10
PCLO		15	3.50	SYNE1		13	4.70	GALNS		2	3.10
LRP1B		15	3.50	UBR4		13	4.70	HSPG2		2	3.10
ADGRV1		15	3.50	SRRM2		13	4.70	AFF3		2	3.10
ATM		14	3.30	DNAH1		13	4.70	MEF2A		2	3.10
DST		14	3.30	DST		12	4.30	MYO1F		2	3.10
KMT2D		14	3.30	CENPF		12	4.30	MUC2	3.72E-12	2	3.10
ARID1A		14	3.30	NEB		12	4.30	MYO7A		2	3.10
FBN2		13	3.00	ARID1A		12	4.30	NFATC1		2	3.10
MUC2		13	3.00	MDN1		12	4.30	NFIA		2	3.10
FMN2		13	3.00	SYNE2		12	4.30	NPHS1		2	3.10
MUC17		13	3.00	PBRM1		12	4.30	PAX4		2	3.10

CCRCC				PRCC				ChRCC			
Gene	MutSig[a]	#Case	Freq[b]	Gene	MutSig[a]	#Case	Freq[b]	Gene	MutSig[a]	#Case	Freq[b]
				BIRC6		12	4.30	PCDH1		2	3.10
				CSMD1		12	4.30	PRODH		2	3.10
				MEGF8		11	4.00	RB1		2	3.10
				LRP2		11	4.00	RYR1		2	3.10
				RYR3		11	4.00	TAL1		2	3.10
				KDM6A		11	4.00	TG		2	3.10
				PCLO		11	4.00	USP9X		2	3.10
				PCF11		11	4.00	TRRAP		2	3.10
				ABCA13		11	4.00	USP14		2	3.10
				BOD1L1		11	4.00	ARHGEF2		2	3.10
				LRBA		10	3.60	ESPL1		2	3.10
				EP300		10	3.60	SLK		2	3.10
				LRP1		10	3.60	HCN4		2	3.10
				RYR1		10	3.60	FAM189B		2	3.10
				RYR2		10	3.60	KDELR3		2	3.10

CCRCC				PRCC				ChRCC			
Gene	MutSig[a]	#Case	Freq[b]	Gene	MutSig[a]	#Case	Freq[b]	Gene	MutSig[a]	#Case	Freq[b]
				SMARCA4		10	3.60	DIDO1		2	3.10
				CUL3		10	3.60	ADAMTS7		2	3.10
				SEC16A		10	3.60	LMTK2		2	3.10
				PRRC2C		10	3.60	RPH3A		2	3.10
				PLXNB2		10	3.60	ZNF521		2	3.10
				LRP1B		10	3.60	HEATR1		2	3.10
				ADGRV1		10	3.60	YLPM1		2	3.10
				HELZ2		10	3.60	AICDA		2	3.10
				CSMD2		10	3.60	KIAA1324		2	3.10
				DYNC1H1		9	3.30	KCNT1		2	3.10
				HSPG2		9	3.30	TSHZ3		2	3.10
				NF2		9	3.30	CSMD1		2	3.10
				PLEC		9	3.30	DDX50		2	3.10
				TERT		9	3.30	DYNC2H1		2	3.10
				DNAH11		9	3.30	BAIAP2L2		2	3.10

CCRCC				PRCC				ChRCC			
Gene	MutSig[a]	#Case	Freq[b]	Gene	MutSig[a]	#Case	Freq[b]	Gene	MutSig[a]	#Case	Freq[b]
				GBF1		9	3.30	C3ORF20		2	3.10
				DOCK4		9	3.30	KIAA1109		2	3.10
				SPEN		9	3.30	ZNF598		2	3.10
				KIF1B		9	3.30	PKD1L2		2	3.10
				CLUH		9	3.30	ZNF831		2	3.10
				SZT2		9	3.30	OR4X1		2	3.10
				NIPBL		9	3.30	OR13C2	3.28E-02	2	3.10
				PRR12		9	3.30				
				CHD8		9	3.30				
				HMCN1		9	3.30				
				WDR81		9	3.30				
				MUC5B		9	3.30				

[a]Q-value

[b]%

Potential actionable targets in TSC-RCC cases

In Case 1, we identified 3 potentially actionable targets. These included *GNA11*, *NOTCH3* and *ZNRF3* for which MAPK pathway inhibitors, gamma secretase inhibitors and porcupine inhibitors can be considered, respectively. In Case 2, there was 1 potentially actionable target. It was *TSC2*, and mTOR inhibitors can be considered for targeted therapy.

Differentially expressed genes in TSC-RCC cases

We assessed 770 genes to identify differentially expressed genes (DEGs). Case 1 includes 20 upregulated and 33 downregulated genes with a 2-fold change, and Case 2 has 202 upregulated and 308 downregulated genes with a 2-fold change. Among those, the *ALK* and *CRLF2* mRNA expression was upregulated, and *CDH1*, *MAP3K1*, *RUNX1*, *SETBP1* and *TSC1* mRNA expression was downregulated in both TSC-RCCs. Cancer-related pathways with DEGs are presented in figure 12 and 13.

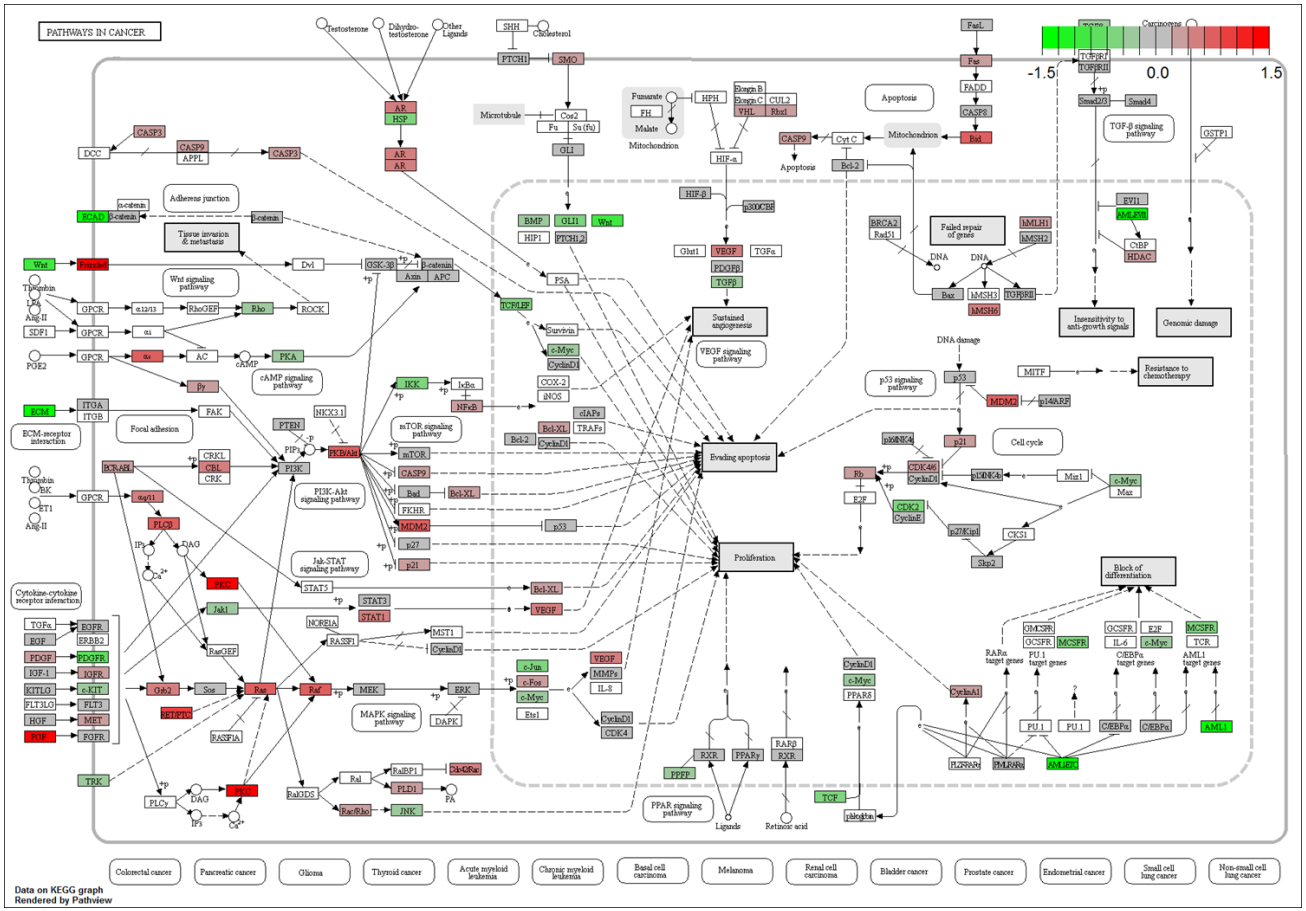

Figure 12. mRNA expression of pan-cancer panel genes in TSC-RCC Case 1

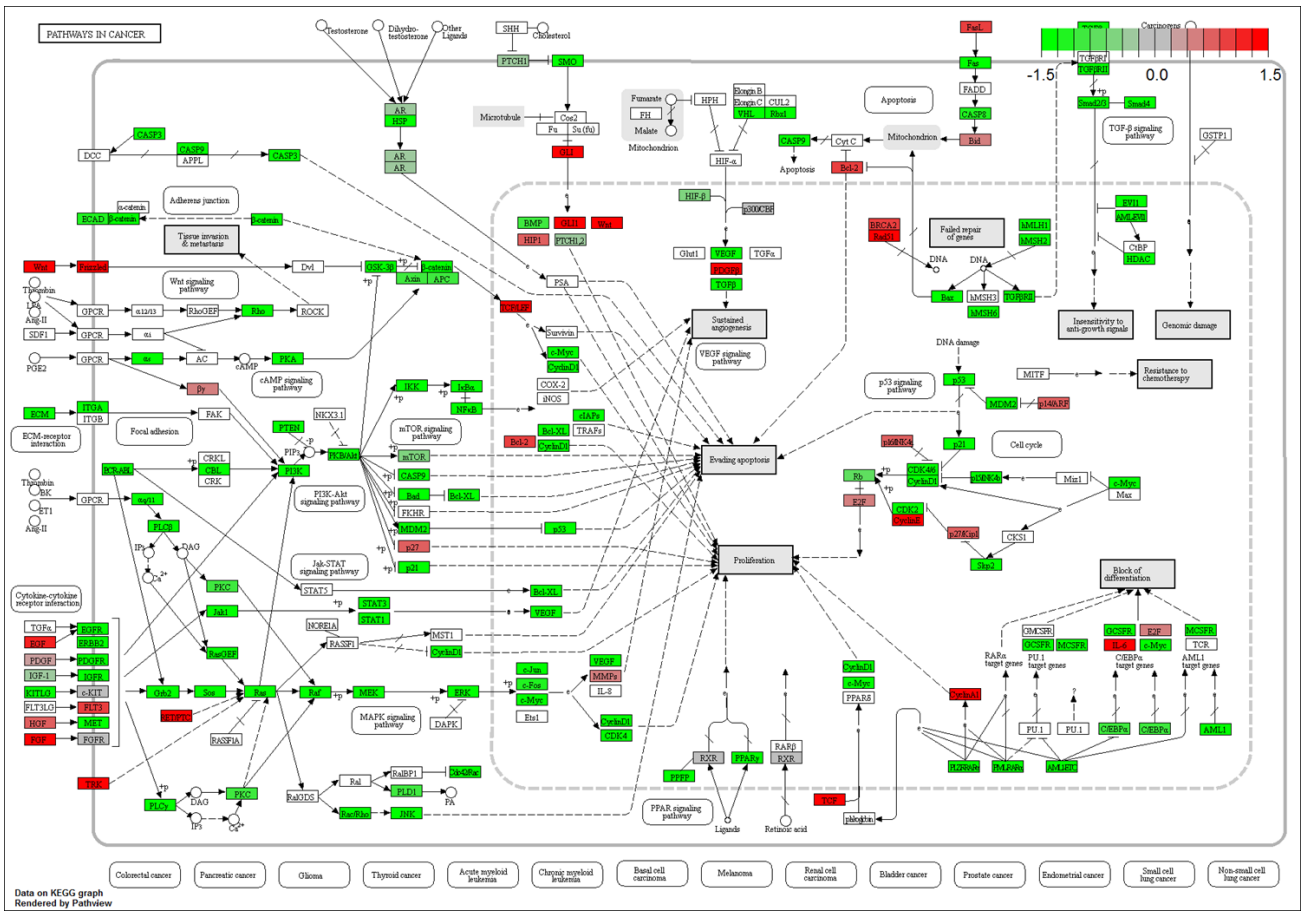

Figure 13. mRNA expression of pan-cancer panel genes in TSC-RCC Case 2

Discussion

The histopathologic features of TSC-RCC have been elucidated (8,9). One study classified them as TSC-associated papillary RCC (52%, 24 cases), HOCT (33%, 15 cases) and unclassified RCC (15%, 7 cases) (9). The authors emphasized the uniformly deficient expression of SDHB in TSC-associated papillary RCC. Another study classified TSC-RCC as RAT-like (30%, 17 cases), chromophobe-like (59%, 34 cases) and eosinophilic/macrocystic RCC (11%, 6 cases) (8). Though those studies classified different histopathologic subtypes, TSC-associated papillary RCC and RAT-like RCC have similar histologic features and could be categorized as RCC with (angio)leiomyomatous stroma (3). Also, HOCT and chromophobe-like RCC could be regarded as one subtype.

The mTOR activation has been thought to one of the pathogenic alterations in TSC-RCC because alterations of *TSC1* or *TSC2* genes were responsible for the development of TSC. However, the pathogenic role of mTOR activation on TSC-RCC pathogenesis has not been studied. We identified mTOR activation by phospho-mTOR immunohistochemistry. Our results suggest that the mTOR pathway is activated and responsible for the

pathogenesis and serves as a rationale for the possible use of mTOR inhibitor in our two patients with TSC-RCC.

We performed WES and reported genetic alterations in TSC-RCC, especially first results of unclassified and eosinophilic/macrocystic RCC. There were genetic analysis of 5 TSC-associated papillary RCC cases from one patient and molecular karyotyping of 15 eosinophilic/macrocystic RCC cases without clinical evidence of TSC (47-49). In TSC-associated papillary RCC cases, there were second hit mutations (3 SNVs, 1 indel and 1 LOH) in *TSC2* and somatic mutations of *PROS1*, *NPFFR2*, *TLL2* and *RASA1* were identified (47). In sporadic cases of eosinophilic/macrocystic RCC, copy number gain of 16p-q, 7p-q, 13q, 19p, 1p and 10q, copy number loss of Xp, 22q, 19p,19q and Xq and LOH in 16p, Xq, 11p and 9q were identified (48,49).

In our cases, the germline mutations of *TSC2* were identified, a *TSC2* nonsense mutation in Case 1 and a *TSC2* splice donor variant mutation in Case 2. For the development of tumours related to TSC, biallelic *TSC2* inactivation is needed. However, we could not find additional *TSC2* mutations or LOH in Case 1. There is the possibility that other types of mutations (large indel or epigenetic alterations), not detected in WES, may exist in the Case 1 patient or *TSC2* inactivation was not responsible for mTOR activation and tumour progression as histopathologic feature of Case 1 was truly unclassifiable. In practice, it is reported that approximately 10-25% of TSC patients have no

TSC1 or *TSC2* mutations detected in conventional genetic testing (11). In Case 2, there was additional *TSC2* somatic mutation.

The somatic mutation analysis showed different genetic mutation profiles from common RCCs. In Case 1, all genetic alterations, except *KMT2C* (in PRCC), *PBRM1* (in CCRCC) and *TTN* (in CCRCC, PRCC and ChRCC), were found with a less than 5% frequency with those in common RCCs. In Case 2, there were no common genes, except the *TG* gene, which showed 3.08% frequency with those in ChRCC. These genetic features support the idea that TSC-RCC should be classified as a distinct entity. Along with previous genetic studies of TSC-associated papillary RCC (47) and sporadic cases of eosinophilic/macrocystic RCC (48,49), our data suggest that TSC-RCC could be listed as an emerging or distinct entity in next edition of WHO classification of tumours of the kidney. The *USP34* and *NDE1* alteration in TSC-associated papillary RCC was found and in Case 1 and 2, respectively.

We aimed to elucidate the pathogenic basis of TSC-RCC. In Case 1, we selected 12 cancer genes and identified 6 pathways. The *CHD8* gene acts as a TSG and is associated with the chromatin remodelling pathway and affects cell survival and cell proliferation. *CHD8* c.2368C>T, p.R790C mutation was previously reported in malignant melanoma and is considered pathogenic based upon FATHMM (36). The pathogenic role on cancer of *CRISPLD1* and *EPB41L4A* genes were not studied well. *CRISPLD1*

c.1363C>T, p.R455* was in LCCL domain and has not been previously reported. Also, *EPB41L4A* c.1618C>T, p.R540C mutation has not been previously reported. The *GNA11* gene is an OG and is a component of GPCR pathway and involved in cell proliferation, invasion and differentiation. *GNA11* c.604C>T, p.R202W mutation located in G-alpha domain has not been previously reported. The *NOTCH3* gene acts as OG and belongs to Notch signalling pathway and is involved in stem-like properties, cell differentiation and proliferation. *NOTCH3* c.1194C>T, p.G398G mutation in EGF_CA domain has previously been reported in urothelial carcinoma of urinary bladder, hepatocellular carcinoma and cutaneous malignant melanoma (39,40). The *PBRM1* gene is a TSG and is a component of chromatin remodelling pathway and is involved in cell cycle progression, invasiveness and stemness. *PBRM1* c.49G>A, p.G17R mutation was previously reported in prostate adenocarcinoma (37,38). The *PTPRU* gene acts as a TSG and affects Wnt/β-catenin pathway and is involved in cell proliferation, focal adhesion and invasiveness. *PTPRU* c.1412G>A, p.R471H mutation was not previously reported. The *RGS12* gene is associated with GPCR pathway, however, the pathogenic role on cancer was not established well. *RGS12* c.4073C>T, p.P1358L mutation was in RGS12_usC domain and was not previously reported. The *SETBP1* gene is an OG and affects PP2A pathway and cell proliferation, apoptosis and cell migration. *SETBP1* c.2572G>A, p.E858K

mutation was previously reported in oesophageal carcinoma, cutaneous malignant melanoma, oesophagus-stomach cancer and haematopoietic neoplasm (36-38). The FATHMM prediction was pathogenic (36). The *SMARCA4* is a TSG and is a component of the chromatin remodelling pathway and is involved in cell cycle progression, invasiveness and stemness. *SMARCA4* c.3067G>A, p.E1023K mutation was in SNF2_N domain and previously reported in colorectal adenocarcinoma and lung cancer (36-38). The *STMN1* gene acts as an OG and affects microtubule dynamics and is involved in cell cycle progression, invasiveness and metastasis. *STMN1* c.235G>A, p.E79K was in Stathmin domain and has not been reported previously. The *ZNRF3* acts as a TSG and affects Wnt/β-catenin pathway and is involved in cell proliferation, apoptosis and invasiveness. *ZNRF3* c.1361G>A, p.R454H has not been previously reported.

In Case 2, we identified 2 cancer genes and pathways. The *IWS1* gene acts as an OG and involved in mRNA processing and tumour growth, migration and invasiveness. *IWS1* c.2048A>G, p.N683S mutation was in Med26 domain and was not previously reported. The *TSC2* gene is thought to be a TSG and is involved in PI3K/AKT/mTOR pathway and affects cell proliferation, metabolism and cell survival. *TSC2* c.1372C>T, p.R458* was in DUF3384 domain and was previously reported in sporadic pulmonary lymphangioleiomyomatosis (36). The FATHMM prediction was pathogenic.

The driver gene mutations in Case 2 were assumed *IWS1* and *TSC2* gene mutations. The concern that only two driver gene mutations are possible and responsible for the development of cancer is arose. Researches dealing with driver gene mutations stated that two to eight driver gene mutations can lead to cancer development and progression and even one driver gene mutations were identified in some types of cancer (33,52-54). In sporadic cases of eosinophilic/macrocystic RCC, there were copy number alterations in multiple chromosomes (48,49). Our Case 2 can be classified histopathologically as eosinophilic/macrocystic RCC and there were much DEGs compared to Case 1. Previous study and our results can be interpreted that Our Case 2 may have copy number alterations and chromosomal imbalance could be responsible for development and progression of eosinophilic/macrocystic RCC.

It is difficult to determine whether the genetic alterations are pathogenic or not. The “20/20 rule” can be a helpful criterion for identifying driver genes (33); however, it cannot tell us whether any mutations that are not well documented are pathogenic. One study evaluated mutational signature patterns and reported >200 each TSGs and OGs (34). However, an aneuploidy pattern without pathogenic features can lead to misinterpretation. The oncogenic *IWS1* gene is predicted as TSG in that study. Mutational features of well-known genes are relatively well documented. For instance,

APC mutations within N-terminal 1600 amino acids are pathogenic, and those within C-terminal 1200 amino acids are not. We identified *APC* mutations in Case 2 and the mutation was in C-terminal side. The β-catenin immunohistochemistry revealed no aberrant nuclear expression, consistent with the absence of any pathogenic effect (data not shown). Features of many other driver genes are still unknown. More specific functional studies with base editing and more representative biologic system studies will provide the proper rationale for patient selection and target therapy.

Validation of aforementioned putative pathogenic pathways would be challenging but necessary and meaningful. As mentioned above, whether the identified genetic alterations are pathogenic or not should be determined first. To this task, base editing using CRISPR (clustered regularly interspaced short palindromic repeat)/Cas9 (55) will be performed and carefully controlled biologic system of experimental animals needed. Another possible method to assess putative pathogenic pathways is performing immunohistochemical study. Actually, we performed phospho-mTOR immunohistochemical staining and identified mTOR pathway activation in both TSC-RCC cases. However, assessment of other putative pathogenic pathways with immunohistochemical study needs further study and has limitations. First, antibody use and research of the antibody is not well established. Second, the pathogenic pathway and upstream and downstream molecules needs to be

elucidated in more detail. Third, the immunostaining of cancer genes can be altered and influenced by other pathways. Forth, other molecular study, such as mRNA sequencing, should be conducted to interpret and reconstruct immunostaining expression results. For these reasons, we could not performed further immunohistochemical study to assess putative pathogenic pathways.

We analysed mRNA expression on 770 genes. Among the cancer genes from TSC-RCC cases, we evaluated *GNA11*, *NOTCH3*, *PBRM1*, *SETBP1*, *SMARCA4* and *STMN1* mRNA expression. *NOTCH3* was upregulated, and *SETBP1* was downregulated with a 2-fold change in Case 1. Among cancers, the *NOTCH3* mRNA expression was upregulated rather than downregulated (36). The *NOTCH3* mRNA expression with our mutation was 26 percentile in hepatocellular carcinoma and 56 percentile in melanoma (37,38). The *SETBP1* mRNA expression was upregulated rather than downregulated in cancers (36). The *SETBP1* mRNA expression with our mutation was 60 percentile in oesophageal carcinoma and 97 percentile in melanoma.

Additionally, in both TSC-RCCs, the mRNA expression of *ALK* and *CRLF2* genes was upregulated, and *CDH1*, *MAP3K1*, *RUNX1*, *SETBP1* and *TSC1* genes were downregulated. The mRNA expression profile would be useful for the molecular classification rather than individual characterization because mRNA expression can vary in identical cancer types. mRNA

expression alone is not sufficient to account for its pathogenic role. Expression can be influenced by genetic mutation, upstream molecules, and interaction with other signalling pathways. Additionally, mRNA expression is not well correlated with protein expression, and upregulation or downregulation does not indicate activation or inactivation. mRNA expression was evaluated in a few genes, and pathogenic pathways cannot be discovered based upon protein-protein interactions.

There are some limitations in our study. First, we evaluated just two cases of TSC-RCC due to rarity of this entity. The population prevalence of TSC is approximately 1 in 20,000 and the occurrence of RCC is about 2-3% of patients (11,56). In archival tissue, we could find only two cases of TSC-RCC among 850 RCCs. Second, tumour purity of Case 1 was low and DNA quality of both cases were relatively low to achieve clear molecular characteristics. Third, we did not perform whole genome sequencing, which could identify large indels, translocations and fusions. Forth, we could not perform mRNA sequencing due to poor RNA quality. Alternatively, we analysed mRNA expression using nanostring. Those limitations should be kept in mind when design and perform further molecular study.

In summary, we assessed the histopathologic features and genetic alterations in two cases of TSC-RCC. The mTOR activation was assessed by phospho-mTOR immunohistochemistry. WES revealed cancer gene

alterations and putative pathogenic pathways that included the chromatin remodelling pathway (*CHD8*, *PBRM1* and *SMARCA4*), GPCR pathway (*GNA11* and *RGS12*), Notch signalling pathway (*NOTCH3*), Wnt/β-catenin pathway (*PTPRU* and *ZNRF3*), PP2A pathway (*SETBP1*) and microtubule dynamics pathway (*STMN1*) in Case 1 and the mRNA processing (*IWS1*) and PI3K/AKT/mTOR pathway (*TSC2*) in Case 2. We evaluated mRNA expression and identified several DEGs, including *ALK*, *CDH1*, *CRLF2*, *MAP3K1*, *RUNX1*, *SETBP1* and *TSC1*. Also, we suggest additional therapeutic agents. We hope our results will help advance our understanding of the pathogenesis of TSC-RCC, design molecular cancer studies and translate cancer research into precision medicine.

References

1. Rini BI, Rathmell WK, Godley P. Renal cell carcinoma. *Curr Opin Oncol* 2008;**20**:300-306.
2. Srigley JR, Delahunt B, Eble JN, Egevad L, Epstein JI, Grignon D, Hes O, Moch H, Montironi R, Tickoo SK, Zhou M, Argani P; ISUP Renal Tumor Panel. The International Society of Urological Pathology (ISUP) Vancouver Classification of Renal Neoplasia. *Am J Surg Pathol* 2013;**37**:1469-1489.
3. Moch H, Amin MB, Argani P, Cheville J, Delahunt B, Martignoni G, Medeiros LJ, Srigley JR, Tan PH, Tickoo SK. Renal cell tumours: Introduction. World Health Organization Classification of Tumours of the Urinary System and Male Genital Organs, 4th Edition. Edited by Moch H, Humphrey PA, Ulbright TM, Reuter VE. Lyon, IARC Press, 2016, pp. 14-17.
4. Edge SB, Byrd DR, Compton CC, Fritz AG, Greene FL, Trotti A. AJCC Cancer Staging Manual, 7th Edition. New York, Springer, 2009, pp. 479-489.
5. Gong J, Gerendash B, Dizman N, Khan A, Pal SK. Advances in treatment of metastatic renal cell carcinoma. *Curr Opin Urol* 2016;**26**:439-446.

6. Weinstock M, McDermott D. Targeting PD-1/PD-L1 in the treatment of metastatic renal cell carcinoma. *Ther Adv Urol* 2015;**7**:365-377.
7. Curtis SA, Cohen JV, Kluger HM. Evolving Immunotherapy Approaches for Renal Cell Carcinoma. *Curr Oncol Rep* 2016;**18**:57.
8. Guo J, Tretiakova MS, Troxell ML, Osunkoya AO, Fadare O, Sangoi AR, Shen SS, Lopez-Beltran A, Mehra R, Heider A, Higgins JP, Harik LR, Leroy X, Gill AJ, Trpkov K, Campbell SC, Przybycin C, Magi-Galluzzi C, McKenney JK. Tuberous sclerosis-associated renal cell carcinoma: a clinicopathologic study of 57 separate carcinomas in 18 patients. *Am J Surg Pathol* 2014;**38**:1457-1467.
9. Yang P, Cornejo KM, Sadow PM, Cheng L, Wang M, Xiao Y, Jiang Z, Oliva E, Jozwiak S, Nussbaum RL, Feldman AS, Paul E, Thiele EA, Yu JJ, Henske EP, Kwiatkowski DJ, Young RH, Wu CL. Renal cell carcinoma in tuberous sclerosis complex. *Am J Surg Pathol* 2014;**38**:895-909.
10. Crino PB, Nathanson KL, Henske EP. The tuberous sclerosis complex. *N Engl J Med* 2006;**355**:1345-1356.
11. Northrup H, Krueger DA; International Tuberous Sclerosis Complex Consensus Group. Tuberous sclerosis complex diagnostic criteria update: recommendations of the 2012 Iinternational Tuberous Sclerosis Complex Consensus Conference. *Pediatr Neurol* 2013;**49**:243-254.

12. Cancer Genome Atlas Research Network. Comprehensive molecular characterization of clear cell renal cell carcinoma. *Nature* 2013;**499**:43-49.
13. Cancer Genome Atlas Research Network. Comprehensive Molecular Characterization of Papillary Renal-Cell Carcinoma. *N Engl J Med* 2016;**374**:135-145.
14. Davis CF, Ricketts CJ, Wang M, Yang L, Cherniack AD, Shen H, Buhay C, Kang H, Kim SC, Fahey CC, Hacker KE, Bhanot G, Gordenin DA, Chu A, Gunaratne PH, Biehl M, Seth S, Kaipparettu BA, Bristow CA, Donehower LA, Wallen EM, Smith AB, Tickoo SK, Tamboli P, Reuter V, Schmidt LS, Hsieh JJ, Choueiri TK, Hakimi AA; Cancer Genome Atlas Research Network, Chin L, Meyerson M, Kucherlapati R, Park WY, Robertson AG, Laird PW, Henske EP, Kwiatkowski DJ, Park PJ, Morgan M, Shuch B, Muzny D, Wheeler DA, Linehan WM, Gibbs RA, Rathmell WK, Creighton CJ. The somatic genomic landscape of chromophobe renal cell carcinoma. *Cancer Cell* 2014;**26**:319-330.
15. Manley BJ, Hakimi AA. Molecular profiling of renal cell carcinoma: building a bridge toward clinical impact. *Curr Opin Urol* 2016;**26**:383-387.
16. Motzer RJ, Escudier B, Oudard S, Hutson TE, Porta C, Bracarda S, Grünwald V, Thompson JA, Figlin RA, Hollaender N, Urbanowitz G,

Berg WJ, Kay A, Lebwohl D, Ravaud A; RECORD-1 Study Group. Efficacy of everolimus in advanced renal cell carcinoma: a double-blind, randomised, placebo-controlled phase III trial. *Lancet* 2008;**372**:449-456.

17. Collins FS, Varmus H. A new initiative on precision medicine. *N Engl J Med* 2015;**372**:793-795.
18. Jameson JL, Longo DL. Precision medicine--personalized, problematic, and promising. *N Engl J Med* 2015;**372**:2229-2234.
19. Moch H, Amin MB, Argani P, Cheville J, Delahunt B, Martignoni G, Medeiros LJ, Srigley JR, Tan PH, and Tickoo SK: In Moch H, Humphrey PA, Ulbright TM, and Reuter VE (eds): Tumours of the kidney. World Health Organization classification of tumours of the urinary system and male genital organs, 4th edition. Lyon: IARC Press, 2016. pp. 11-76
20. Moch H, Amin MB, Argani P, Cheville J, Delahunt B, Martignoni G, Medeiros LJ, Srigley JR, Tan PH, and Tickoo SK: In Moch H, Humphrey PA, Ulbright TM, and Reuter VE (eds): Renal cell tumours: introduction. World Health Organization classification of tumours of the urinary system and male genital organs, 4th edition. Lyon: IARC Press, 2017. pp. 14-17
21. Delahunt B, Cheville JC, Martignoni G, Humphrey PA, Magi-Galluzzi C, McKenney J, Egevad L, Algaba F, Moch H, Grignon DJ, Montironi R, Srigley JR; Members of the ISUP Renal Tumor Panel. The

International Society of Urological Pathology (ISUP) grading system for renal cell carcinoma and other prognostic parameters. *Am J Surg Pathol* 2013;**37**:1490-1504.

22. Rini BI, McKiernan JM, Chang SS, Choueiri TK, Kenney PA, Landman J, Leibovich BC, Tickoo SK, Vikram R, Zhou M, Stadler WM: In Amin MB, Edge SB, Greene FL, Byrd DR, Brookland RK, Washington MK, Gershenwald JE, Compton CC, Hess KR, Sullivan DC, Jessup JM, Brierley JD, Gaspar LE, Schilsky RL, Balch CM, Winchester DP, Asare EA, Madera M, Gress DM, Meyer LR (eds): Kidney. AJCC Cancer Staging Manual 8th Edition. Chicago, IL: Springer, 2016. pp. 739-748
23. Andrews S. FastQC. A quality control tool for high throughput sequence data. http://www.bioinformatics.bbsrc.ac.uk/projects/fastqc/ 2010.
24. Li H, Durbin R. Fast and accurate short read alignment with Burrows-Wheeler transform. *Bioinformatics* 2009;**25**:1754-1760.
25. McKenna, A, Hanna M, Banks E, Sivachenko A, Cibulskis K, Kernytsky A, Garimella K, Altshuler D, Gabriel S, Daly M, DePristo MA. The Genome Analysis Toolkit: a MapReduce framework for analyzing next-generation DNA sequencing data. *Genome Res* 2010;**20**:1297-1303.
26. Cingolani P, Platts A, Wang le L, Coon M, Nguyen T, Wang L, Land SJ, Lu X, Ruden DM. A program for annotating and predicting the effects of single nucleotide polymorphisms, SnpEff: SNPs in the genome of

Drosophila melanogaster strain w1118; iso-2; iso-3. *Fly (Austin)* 2012;**6**:80-92.

27. Cibulskis K, Lawrence MS, Carter SL, Sivachenko A, Jaffe D, Sougnez C, Gabriel S, Meyerson M, Lander ES, Getz G. Sensitive detection of somatic point mutations in impure and heterogeneous cancer samples. *Nat Biotechnol* 2013;**31**:213-219.
28. Saunders CT, Wong WS, Swamy S, Becq J, Murray LJ, Cheetham RK. Strelka: accurate somatic small-variant calling from sequenced tumor-normal sample pairs. *Bioinformatics* 2012;**28**:1811-1817.
29. Ramos AH, Lichtenstein L, Gupta M, Lawrence MS, Pugh TJ, Saksena G, Meyerson M, Getz G. Oncotator: cancer variant annotation tool. *Hum Mutat* 2015;**36**:E2423-9.
30. Adzhubei IA, Schmidt S, Peshkin L, Ramensky VE, Gerasimova A, Bork P, Kondrashov AS, Sunyaev SR. A method and server for predicting damaging missense mutations. *Nat Methods* 2010;**7**:248-249.
31. Reva B, Antipin Y, Sander C. Predicting the functional impact of protein mutations: application to cancer genomics. *Nucleic Acids Res* 2011;**39**:e118.
32. Schwarz JM, Cooper DN, Schuelke M, Seelow D. MutationTaster2: mutation prediction for the deep-sequencing age. *Nat Methods* 2014;**11**:361-362.

33. Vogelstein B, Papadopoulos N, Velculescu VE, Zhou S, Diaz LA Jr, Kinzler KW. Cancer genome landscapes. *Science* 2013;**339**:1546-1558.
34. Davoli T, Xu AW, Mengwasser KE, Sack LM, Yoon JC, Park PJ, Elledge SJ. Cumulative haploinsufficiency and triplosensitivity drive aneuploidy patterns and shape the cancer genome. *Cell* 2013;**155**:948-962.
35. Kandoth C, McLellan MD, Vandin F, Ye K, Niu B, Lu C, Xie M, Zhang Q, McMichael JF, Wyczalkowski MA, Leiserson MDM, Miller CA, Welch JS, Walter MJ, Wendl MC, Ley TJ, Wilson RK, Raphael BJ, Ding L. Mutational landscape and significance across 12 major cancer types. *Nature* 2013;**502**:333-339.
36. Forbes SA, Beare D, Gunasekaran P, Leung K, Bindal N, Boutselakis H, Ding M, Bamford S, Cole C, Ward S, Kok CY, Jia M, De T, Teague JW, Stratton MR, McDermott U, Campbell PJ. COSMIC: exploring the world's knowledge of somatic mutations in human cancer. *Nucleic Acids Res* 2015;**43**:D805-11.
37. Cerami E, Gao J, Dogrusoz U, Gross BE, Sumer SO, Aksoy BA, Jacobsen A, Byrne CJ, Heuer ML, Larsson E, Antipin Y, Reva B, Goldberg AP, Sander C, Schultz N. The cBio cancer genomics portal: an open platform for exploring multidimensional cancer genomics data. *Cancer Discov* 2012;**2**:401-404.

38. Gao J, Aksoy BA, Dogrusoz U, Dresdner G, Gross B, Sumer SO, Sun Y, Jacobsen A, Sinha R, Larsson E, Cerami E, Sander C, Schultz N. Integrative analysis of complex cancer genomics and clinical profiles using the cBioPortal. *Sci Signal* 2013;**6**:pl1.

39. Kanehisa M, Goto S. KEGG: kyoto encyclopedia of genes and genomes. *Nucleic Acids Res* 2000;**28**:27-30.

40. Kanehisa M, Sato Y, Kawashima M, Furumichi M, Tanabe M. KEGG as a reference resource for gene and protein annotation. *Nucleic Acids Res* 2016;**44**:D457-462.

41. Robinson JT, Thorvaldsdóttir H, Winckler W, Guttman M, Lander ES, Getz G, Mesirov JP. Integrative genomics viewer. Nat Biotechnol. 2011;29:24-26.

42. Thorvaldsdóttir H, Robinson JT, Mesirov JP. Integrative Genomics Viewer (IGV): high-performance genomics data visualization and exploration. Brief Bioinform. 2013;14:178-192.

43. Boeva V, Popova T, Bleakley K, Chiche P, Cappo J, Schleiermacher G, Janoueix-Lerosey I, Delattre O, Barillot E. Control-FREEC: a tool for assessing copy number and allelic content using next-generation sequencing data. Bioinformatics 2012;**28**:423-425.

44. Sathirapongsasuti JF, Lee H, Horst BA, Brunner G, Cochran AJ, Binder S, Quackenbush J, Nelson SF. Exome sequencing-based copy-number

variation and loss of heterozygosity detection: ExomeCNV. Bioinformatics 2011;**27**:2648-2654.

45. Krämer A, Green J, Pollard J Jr, Tugendreich S. Causal analysis approaches in Ingenuity Pathway Analysis. *Bioinformatics* 2014;**30**:523-530.

46. Szklarczyk D, Franceschini A, Wyder S, Forslund K, Heller D, Huerta-Cepas J, Simonovic M, Roth A, Santos A, Tsafou KP, Kuhn M, Bork P, Jensen LJ, von Mering C. STRING v10: protein-protein interaction networks, integrated over the tree of life. *Nucleic Acids Res* 2015;**43**:D447-452.

47. Tyburczy ME, Jozwiak S, Malinowska IA, Chekaluk Y, Pugh TJ, Wu CL, Nussbaum RL, Seepo S, Dzik T, Kotulska K, Kwiatkowski DJ. A shower of second hit events as the cause of multifocal renal cell carcinoma in tuberous sclerosis complex. *Hum Mol Genet* 2015;**24**:1836-1842.

48. Trpkov K, Hes O, Bonert M, Lopez JI, Bonsib SM, Nesi G, Comperat E, Sibony M, Berney DM, Martinek P, Bulimbasic S, Suster S, Sangoi A, Yilmaz A, Higgins JP, Zhou M, Gill AJ, Przybycin CG, Magi-Galluzzi C, McKenney JK. Eosinophilic, Solid, and Cystic Renal Cell Carcinoma: Clinicopathologic Study of 16 Unique, Sporadic Neoplasms Occurring in Women. *Am J Surg Pathol* 2016;**40**:60-71.

49. Trpkov K, Abou-Ouf H, Hes O, Lopez JI, Nesi G, Comperat E, Sibony M, Osunkoya AO, Zhou M, Gokden N, Leroy X, Berney DM, Werneck Cunha I, Musto ML, Athanazio DA, Yilmaz A, Donnelly B, Hyndman E, Gill AJ, McKenney JK, Bismar TA. Eosinophilic Solid and Cystic Renal Cell Carcinoma (ESC RCC): Further Morphologic and Molecular Characterization of ESC RCC as a Distinct Entity. *Am J Surg Pathol* 2017;**41**:1299-1308.

50. Meric-Bernstam F, Johnson A, Holla V, Bailey AM, Brusco L, Chen K, Routbort M, Patel KP, Zeng J, Kopetz S, Davies MA, Piha-Paul SA, Hong DS, Eterovic AK, Tsimberidou AM, Broaddus R, Bernstam EV, Shaw KR, Mendelsohn J, Mills GB. A decision support framework for genomically informed investigational cancer therapy. *J Natl Cancer Inst* 2015;**107**.

51. Martignoni G, Pea M, Rocca PC, Bonetti F. Renal pathology in the tuberous sclerosis complex. *Pathology* 2003;**35**:505-512.

52. Tomasetti C, Marchionni L, Nowak MA, Parmigiani G, Vogelstein B. Only three driver gene mutations are required for the development of lung and colorectal cancers. *Proc Natl Acad Sci U S A* 2015;112:118-123.

53. Martincorena I, Raine KM, Gerstung M, Dawson KJ, Haase K, Van Loo P, Davies H, Stratton MR, Campbell PJ. Universal Patterns of Selection in Cancer and Somatic Tissues. *Cell* 2017;**171**:1029-1041.

54. Bailey MH, Tokheim C, Porta-Pardo E, Sengupta S, Bertrand D, Weerasinghe A, Colaprico A, Wendl MC, Kim J, Reardon B, Ng PK, Jeong KJ, Cao S, Wang Z, Gao J, Gao Q, Wang F, Liu EM, Mularoni L, Rubio-Perez C, Nagarajan N, Cortés-Ciriano I, Zhou DC, Liang WW, Hess JM, Yellapantula VD, Tamborero D, Gonzalez-Perez A, Suphavilai C, Ko JY, Khurana E, Park PJ, Van Allen EM, Liang H; MC3 Working Group; Cancer Genome Atlas Research Network, Lawrence MS, Godzik A, Lopez-Bigas N, Stuart J, Wheeler D, Getz G, Chen K, Lazar AJ, Mills GB, Karchin R, Ding L. Comprehensive Characterization of Cancer Driver Genes and Mutations. *Cell* 2018;**173**:371-385.

55. Ran FA, Hsu PD, Lin CY, Gootenberg JS, Konermann S, Trevino AE, Scott DA, Inoue A, Matoba S, Zhang Y, Zhang F. Double nicking by RNA-guided CRISPR Cas9 for enhanced genome editing specificity. *Cell* 2013;**154**:1380-1389.

56. Henske EP, Jóźwiak S, Kingswood JC, Sampson JR, Thiele EA. Tuberous sclerosis complex. *Nat Rev Dis Primers* 2016;**2**:16036.

국문 초록

목적: 결절성 경화증 연관 신세포암은 독특한 임상 및 조직병리학적 특징을 가지고 있으며 신세포암의 특별한 형태로 고려되고 있다. 결절성 경화증은 *TSC1* 또는 *TSC2* 유전자의 이상에 의해 발생한다. 본 연구의 목적은 *TSC1* 또는 *TSC2* 유전자의 이상에 의한 mTOR 경로의 활성화를 평가하고 결절성 연관 신세포암의 분자유전학적 특징 및 발생기전을 탐구하고자 하는 것이다.

방법 및 결과: 두 증례의 결절성 경화증 연관 신세포암을 평가하였다. 한 증례는 31 세 여성이었고 다른 증례는 8 세 남아였다. 면역조직화학염색 검사를 통해 mTOR 경로의 활성화를 평가하였다. 전장 엑솜 염기서열분석을 통해 유전적 돌연변이를 검색하였으며 발생기전을 분석하였다. NanoString Technologies 의 nCounter platform 을 이용하여 차별 발현 유전자를 평가하였다. 그 결과, 두 증례 모두에서 mTOR 경로의 활성화와 *TSC2* 유전자의 생식세포 돌연변이를 확인하였다. 전장 엑솜 염기서열분석에서

몇몇 암 유전자의 돌연변이를 확인하였다. 첫 번째 증례에서는 *CHD8*, *CRISPLD1*, *EPB41L4A*, *GNA11*, *NOTCH3*, *PBRM1*, *PTPRU*, *RGS12*, *SETBP1*, *SMARCA4*, *STMN1*, *ZNRF3* 유전자의 돌연변이를, 두 번째 증례에서는 *IWS1*, *TSC2* 유전자의 돌연변이가 관찰되었다. 더 나아가, 추정적인 발생기전을 평가하였다. 첫 번째 증례에서는 염색질 재구성, G 단백-결합 수용체, NOTCH 신호전달, Wnt/β-catenin, PP2A, 미세소관 동역학 경로가, 두 번째 증례에서는 mRNA 가공, PI3K/AKT/mTOR 경로가 발생기전으로 평가되었다. 또한 *ALK*, *CRLF2* 발현이 두 증례에서 모두 증가되었고 *CDH1*, *MAP3K1*, *RUNX1*, *SETBP1*, *TSC1* 발현이 두 증례에서 모두 감소되었다.

***결론*:** 본 연구를 통해, 결절성 경화증 연관 신세포암에서 mTOR 경로의 활성화, 분자유전학적 특징 및 유전적 발생 경로를 밝혔다. 이를 바탕으로 결절성 경화증 연관 신세포암의 발생기전에 대해 보다 깊이 이해할 수 있을 것으로 생각된다.

Acknowledgement

I would like to express my deep gratitude to my teachers and family. This dissertation could not have been written without them. My deepest gratitude goes to my mentor, Professor Kyung Chul Moon, who has taught me not only knowledge, but also proper attitude as a doctor and a researcher. I also would like to thank my committee members for helpful discussions on this dissertation.